Ergodic Secrecy Rate of Optimal Source-Destination Pair Selection in Frequency-Selective Fading

Shashi Bhushan Kotwal, *Student Member, IEEE*, Chinmoy Kundu, *Member, IEEE*, Sudhakar Modem, *Member, IEEE*, Ankit Dubey, *Member, IEEE*, and Mark F. Flanagan, *Senior Member, IEEE*

Abstract-Node selection is a simple technique to achieve diversity and thereby enhance the physical layer security in future wireless communication systems which require low complexity. High-speed data transmission often encounters frequency selective fading. In this context, we evaluate the exact closed-form expression for the ergodic secrecy rate (ESR) of the optimal sourcedestination pair selection scheme with single-carrier cyclic-prefix modulation, where the destination and eavesdropper channels both exhibit independent frequency selective fading with an arbitrary number of multipath components. A simplified analysis in the high-SNR scenario along with an asymptotic analysis is also provided. We also derive and compare the corresponding results for the sub-optimal source-destination pair selection scheme. We show that our analysis produces the corresponding ESR results under narrowband independent Nakagami-m fading channel with any arbitrary integer parameter m. The effect of transmitters, destination and eavesdropping paths correlation on the ESR is also demonstrated. Our solution approach is general and can be used to find the ESR of a wider variety of transmitter selection schemes.

Index Terms—Ergodic secrecy rate, frequency selective fading, Nakagami-m fading, source-destination pair selection, asymptotic analysis.

I. INTRODUCTION

In future wireless networks, e.g. internet-of-things (IoT), where low-complexity nodes are preferable, physical layer security (PLS) may be a suitable choice for implementing data security with its relatively simple channel coding techniques, instead of implementing complex higher-layer encryption techniques [1]. Improving PLS through the diversity gain achieved by an antenna, transmitter/source, relay, destination, and/or source-destination pair selection technique is a relatively simple method suitable for implementation in low-complexity dense and heterogeneous future networks, and has been studied extensively in [2]–[15]. The authors in [2]–[12] considered only source or relay selection schemes. Other works considered joint source-relay pair [14], [15] or relay-destination pair selection [13] in a multiple relay/destination scenario.

Other works considered joint relay-destination pair selection [13] or source-relay pair [14], [15] selection in a multiple source/relay/destination scenario. In situations where only source to destination channel(s) state information (CSI) was

Shashi Bhushan Kotwal, Sudhakar Modem, and Ankit Dubey are with Indian Institute of Technology Jammu, India (email: {shashi.kotwal, sudhakar.modem, ankit.dubey}@iitjammu.ac.in).

Chinmoy Kundu and Mark F. Flanagan are with University College Dublin, Ireland (email: chinmoy.kundu@ucd.ie and mark.flanagan@ieee.org).

This publication has emanated from research supported in part by Science Foundation Ireland (SFI) under Grant Number 17/US/3445 and is co-funded under the European Regional Development Fund under Grant Number 13/RC/2077, and by Science and Engineering Research Board, India sponsored project ECR/2018/002795.

available, the authors in [2]–[5], [12]–[15] implemented suboptimal node selection scheme. In addition to the source to destination CSI, the authors in [6]–[11] assumed availability of the source to eavesdropper CSI and implemented an optimal node selection scheme. The sub-optimal selection scheme is aimed at maximizing the source to destination channel rate, whereas the optimal selection scheme maximizes the overall secrecy rate of the system. Moreover, it can provide a theoretical upper bound on the performance of sub-optimal selection schemes.

As PLS exploits the random behaviour of the channel, the nature of channel fading, i.e., narrowband flat fading or frequency selective fading, affects the performance of each selection scheme differently. Most of the literature on node selection for security is studied in the context of a narrowband flat fading channel [2], [3], [6]–[10]. In these papers, the secrecy outage probability (SOP) is generally considered as the principal performance metric. The authors in [2], [3] extended the SOP analysis to ergodic secrecy rate (ESR) analysis for a transmitter selection scheme in a Nakagami-m fading environment. Although the authors presented a closed-form solution, the scheme is sub-optimal. Moreover, the authors in [3] did not provide an exact ESR analysis, but an upper bound; also, high-SNR and asymptotic analysis were not provided. SOP and ESR analysis of a sub-optimal transmitter antenna selection in a relayed network with maximal-ratio combining (MRC) at the relay, destination, and eavesdropper was performed in [4] assuming outdated CSI. The authors showed that system secrecy performance degrades in the presence of outdated CSI. The analysis of optimal selection is absent in [4] and the methodology adopted for the ESR analysis in the sub-optimal selection scheme is also different from our work. The authors showed that outdated CSI degrades the secrecy performance. The authors in [8] analyzed the SOP for both the sub-optimal selection and optimal selection schemes in a cognitive radio network. However, the exact ESR for the optimal selection scheme was not presented. The optimal selection scheme was also implemented in [9] on the same system as that of [8] using machine learning techniques; however, no theoretical analysis was presented. Only recently, the ESR of the optimal selection scheme in the presence of multiple eavesdroppers was presented in [10] under Rayleigh fading channel conditions. However, the authors neither analyzed the performance of the source-destination pair selection schemes nor considered frequency selective fading channel conditions.

High-speed wireless data transmission often encounters multipath frequency selective fading in practice. In this scenario, single carrier-cyclic prefix (SC-CP) signaling has been proposed as a solution to overcome the effects of inter-symbol interference (ISI) [16]. Using SC-CP in a frequency selective fading channel, the authors in [5], [11]-[15] considered PLS enhancement through transmitter selection. In a cooperative communication with wireless backhaul involving a single relay and destination, and multiple eavesdroppers, the authors in [5] derived the ESR (including performing an asymptotic analysis) for a sub-optimal selection scheme where the selection was performed on the basis of the transmitter to relay channel quality. In a cooperative communications scenario with multiple relays, multiple destinations, and multiple eavesdroppers, a two-stage joint relay-destination pair selection scheme was proposed in [13], where the relay was selected to minimize the eavesdropping rate. Although ESR is evaluated, the selection scheme is not aimed at maximizing the secrecy capacity of the system, and is therefore sub-optimal. A system with wireless backhaul was considered in [14], where a sub-optimal transmitter-relay pair selection scheme is implemented in the presence of multiple eavesdroppers; here selection was on the basis of maximizing the source to destination channel rate. To degrade the eavesdropping channel with the help of a jammer in the presence of multiple eavesdroppers in a system including wireless backhaul, a two-stage transmitter-relay pair selection scheme was proposed in [15]; this selection scheme was also sub-optimal. Only recently, the authors in [11] introduced the optimal selection scheme for the context of a frequency selective fading channel. However, the authors consider the SOP as the performance metric, not the ESR.

The authors in [17], [18] present the SOP analysis of transmitter antenna selection with correlated channels. The authors in [17] assume receive antenna correlation at the destination and eavesdropper. It is shown that the receive antenna correlation is detrimental to the secrecy performance. The authors in [18] consider correlation between destination and eavesdropper channels, and showed that correlation between destination and eavesdropper channels is beneficial to the SOP performance at high SNR. These papers do not consider frequency selective channel fading and the ESR performance also not considered. If the scattering clusters causing multipath components are at a large distance from the transmitter but in a narrow angular range of it, path correlation can be separated from transmitter/transmit antenna correlation [19]. The authors in [19] showed that in frequency selective channels, the transmitter and receiver antenna correlation along with path correlation have a detrimental effect on the channel capacity. However, the effect of path correlation on the secrecy rate in frequency selective fading channel is unexplored.

In next-generation dense heterogeneous networks, multiple source radio nodes need to serve multiple receive radio nodes simultaneously. The source nodes may actually be acting as relaying nodes for the next level of receiving nodes in a multihop communication setup. In this scenario, choosing the best forwarding path among all possible available paths in order to maximize secrecy is required [13]–[15]. Another practical scenario in which adaptive source-destination pair scheduling is implemented maximising the secrecy of the system is described in [20]–[22]. However, in these scenarios, to the best of the author's knowledge, the ESR performance of the optimal source-destination pair selection (OS) scheme in frequency

selective fading conditions is unavailable. Moreover, the effect of transmitter and path correlation on the ESR performance is not available in the literature. Moreover, the effect of transmitter and path correlation on the ESR performance is not available in the literature. This motivates us to consider the OS scheme and sub-optimal source-destination pair selection (SS) scheme in frequency selective channels.

The system models and the sub-optimal selection schemes in [5], [13]-[15] are different from that considered in this paper. The two-stage transmitter-relay pair selection scheme in [13] does not consider the maximum source to destination channel rate, and a high-SNR analysis is also not presented as in this paper. The work in [5] involves relaying, and the selection is based on the transmitter to relay channel only. Hence, the selection scheme is different from our work, as it does not consider the maximum source to destination channel rate (also note that our results cannot be directly derived from [5]). The system in [14] also involves relaying, and as a result, the system is different from that considered in this paper; the asymptotic analysis of the ESR is also absent. In another two-stage transmitter-relay pair selection scheme (notoptimal) in [15], the transmitter in the first stage is selected based on source to relay channel rate instead of the source to destination channel rate as in our work. Also, the asymptotic analysis of the ESR is presented in integral form instead of closed form. Although the authors in [11] analyze a transmitter selection scheme in frequency selective channel with SC-CP for both optimal and sub-optimal selection schemes, in contrast to our paper, it does not consider either source-destination pair selection or ESR analysis.

- For the first time in the literature, we obtain the exact closed-form ESR for the OS scheme in a frequency selective fading channel with SC-CP modulation in a system consisting of multiple transmitters, multiple destinations, and an eavesdropper. The generalized expressions apply to an arbitrary number of transmitters and destinations, and an arbitrary number of multipath components in the destination and eavesdropper channels.
- We also derive the exact closed-form ESR of the SS scheme and compare it with that of the OS scheme.
- To reduce the computational complexity of the ESR and to find better insights, we derive a high-SNR approximation and asymptotic analysis of the ESR for both OS and SS schemes. We show that it is better for the system secrecy to increase the number of transmitters than the number of destinations in case of the OS scheme, whereas in case of the SS scheme, the ESR shows the same dependence on the number of transmitters as on the number of destinations.
- To derive the ESR, we adopt a completely new approach with respect to the existing literature, which makes use of the cumulative distribution function (CDF) of the ratio of the destination to eavesdropper channel SNR. The method is general and can also be used to derive the ESR of a wide variety of node selection schemes schemes, such as those presented in [5], [13]–[15], [23].
- · We demonstrate numerically the effect of transmitter,

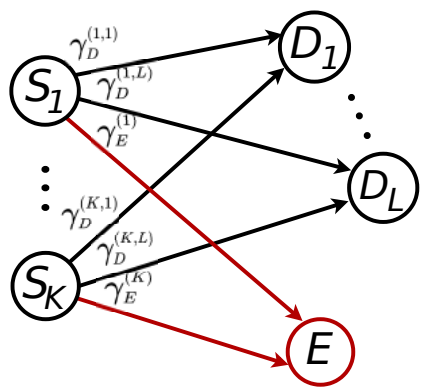


Fig. 1: System model consisting of K transmitters, L legitimate destinations and an eavesdropper.

destination and eavesdropper path correlation on the ESR of the OS and SS schemes. We conclude that correlation among transmitters is detrimental to the ESR performance, while path correlation improves it.

The rest of the paper is organized as follows. The system model is described in Section II. The ESR of the OS scheme, together with its high-SNR and asymptotic analysis, are provided in Section III, while the corresponding analyses for the SS scheme are provided in Section IV. The transmitter and path correlation models are presented in Section V. Results and discussions are presented in Section VI and conclusions are drawn in Section VII.

Notation: ||h|| denotes the Euclidean norm of a vector **h**, $|\mathcal{A}|$ denotes size of set \mathcal{A} , $\mathbb{P}[\cdot]$ denotes the probability of an event, \otimes and $\mathbb{E}\left[\cdot\right]$ denote the Kronecker product and expectation operator respectively, $vec\{\cdot\}$, T and H denote vectorization, transpose and Hermitian operator, respectively. $\Gamma(x) = \int_0^\infty t^{z-1} \exp(-t) dt$ denotes the complete Gamma function, while $\gamma(z,x) = \int_0^x t^{z-1} \exp(-t) dt$ and $\Gamma(z,x) = \int_0^\infty t^{z-1} \exp(-t) dt$ $\int_{x}^{\infty} t^{z-1} \exp(-t) dt$ denote the lower and upper incomplete Gamma function respectively. The probability density function (PDF) and the cumulative distribution function (CDF) of a random variable X are denoted by $f_X(\cdot)$ and $F_X(\cdot)$, respectively.

II. SYSTEM MODEL

We assume that K transmitters S_k , where $k \in \mathcal{S}$ = $\{1,\ldots,K\}$, are transmitting data to L legitimate destinations D_l , where $l \in \mathcal{D} = \{1, \dots, L\}$, through wireless channels in the presence of a passive eavesdropper E. We consider SC-CP modulation at each transmitter, assuming a frequency selective fading channel between each pair of nodes. Due to the multipath propagation, the destination channel S_k - D_l for each $k \in \mathcal{S}$ and $l \in \mathcal{D}$, and the eavesdropping channel S_k -E for each $k \in \mathcal{S}$, contain M_D and M_E paths, respectively. The destination channel $\mathbf{h}_D^{(k,l)} \in \mathbb{C}^{1 \times M_D}$ between S_k - D_l is modelled as a circularly symmetric complex Gaussian random vector of length M_D with zero mean and identity covariance matrix. Similarly, the eavesdropping channel $\mathbf{h}_E^{(\vec{k})} \in \mathbb{C}^{1 imes M_E}$ between S_k -E is also modelled as a circularly symmetric complex Gaussian random vector of length M_E with zero mean and identity covariance matrix. Therefore, the channel coefficient $h_D^{(k,l)}(i)$ for each path $i \in \{1,2,\ldots,M_D\}$, as well as $h_E^{(k)}(i)$ for each path $i \in \{1,2,\ldots,M_E\}$, is an

independent circularly symmetric complex Gaussian random variable with zero mean and unit variance, and its magnitude follows a Rayleigh distribution. We also assume that the channels $\mathbf{h}_D^{(k,\bar{l})}$, for all k and l are are independent and identically distributed (i.i.d.). Similarly channels $\mathbf{h}_{E}^{(k)}$, for all k are also i.i.d. However, the parameters of the distribution of the channels $\mathbf{h}_D^{(k,l)}$ and $\mathbf{h}_E^{(k)}$ are assumed to be different, in general. Owing to SC-CP modulation, the SNRs for each S_k - D_l and S_k -E channel are written as [13]

$$\gamma_D^{(k,l)} = \frac{a_D P_T}{\sigma_D^2} ||\mathbf{h}_D^{(k,l)}||^2 \tag{1}$$

and

$$\gamma_E^{(k)} = \frac{a_E P_T}{\sigma_E^2} ||\mathbf{h}_E^{(k)}||^2, \tag{2}$$

respectively, where P_T is the transmitted power, a_D and a_E are the path loss factors which are inversely proportional to the S_k - D_l and S_k -E distance respectively for each k and l, σ_D^2 and σ_E^2 are the average noise powers at D_l and E, respectively. The PDF of $\gamma_D^{(k,l)}$ follows a Gamma distribution as [13]

$$f_{\gamma_D^{(k,l)}}(x) = \frac{x^{M_D - 1} \exp(-\frac{x}{a_D P_T / \sigma_D^2})}{(a_D P_T / \sigma_D^2)^{M_D} \Gamma(M_D)} = \frac{x^{M_D - 1} \exp(-\frac{x}{\lambda_D})}{\lambda_D^{M_D} \Gamma(M_D)},$$
(3)

where $\lambda_D = a_D P_T / \sigma_D^2$. As observed in [11], the underlying frequency selective channel upon SC-CP modulation behaves as a narrowband Nakagami-m fading channel with integer shape parameter $m=M_D$, and scale parameter representing average SNR $\mathbb{E}[\gamma_D^{(k,l)}]=M_D\lambda_D$, where the average SNR per multipath component is λ_D . As the channel behaves as a Nakagami channel, the ESR performance derived for the OS and SS schemes in this paper is also applicable for the Nakagami fading channel¹ in the similar system assumptions (note that this analysis is not currently available in the literature). As Rayleigh fading is a particular case of Nakagami-m fading when shape parameter m=1, the results derived in this paper also apply to the Rayleigh fading channel. The CDF of $\gamma_D^{(k,l)}$ is in the form of an incomplete Gamma

$$F_{\gamma_D^{(k,l)}}(x) = \int_0^x \frac{y^{M_D - 1} \exp\left(-\frac{y}{\lambda_D}\right)}{\lambda_D^{M_D} \Gamma(M_D)} dy = \frac{\gamma\left(M_D, \frac{x}{\lambda_D}\right)}{\Gamma(M_D)}.$$
(4)

As M_D is an integer, the CDF of $\gamma_D^{(k,l)}$ can be written as [25,

$$F_{\gamma_D^{(k,l)}}(x) = 1 - \exp\left(-\frac{x}{\lambda_D}\right) \sum_{m=0}^{M_D - 1} \frac{1}{m!} \left(\frac{x}{\lambda_D}\right)^m.$$
 (5)

¹The Rayleigh faded channel with L-branch maximal ratio combining (MRC) results in Nakagami fading with shape parameter m = L. Further, the MRC combining L-branch Nakagami-m faded signals results in another Nakagami faded signal with shape parameter mL [24]. Therefore, the analysis provided in this paper can be thought of as a generalized solution that can lead also to solutions for the Nakagami fading context

The PDF and CDF of $\gamma_E^{(k)}$ can be expressed by replacing D with E and (k,l) with (k) in (3) and (5), respectively. We assume that the destination and eavesdropper channels are non-identical, i.e., λ_D and M_D are not necessarily equal to λ_E and M_E , respectively. The secrecy rate achievable for the k^{th} transmitter- l^{th} destination pair in bits per channel use (bpcu) is defined as [26]

$$C_S^{(k,l)} = \left[\log_2\left(\Gamma_S^{(k,l)}\right)\right]^+,\tag{6}$$

where

$$\Gamma_S^{(k,l)} = \frac{1 + \gamma_D^{(k,l)}}{1 + \gamma_E^{(k)}}. (7)$$

The corresponding ESR is then evaluated as [10]

$$C_{\text{erg}}^{(k,l)} = \mathbb{E}\left[C_S^{(k,l)}\right] = \frac{1}{\ln(2)} \int_1^\infty \ln(x) f_{\Gamma_S^{(k,l)}}(x) dx.$$
 (8)

By changing the order of integration and after performing some mathematical manipulations, $C_{erg}^{(k)}$ is reformulated to utilize the CDF of $\Gamma_S^{(k,l)}$ as

$$C_{\text{erg}}^{(k,l)} = \frac{1}{\ln(2)} \int_{1}^{\infty} \frac{1 - F_{\Gamma_{S}^{(k,l)}}(x)}{x} dx. \tag{9}$$

The ESR evaluation using (9) is simpler than using (8), as (9) does not require derivation of the PDF $f_{\Gamma^{(k,l)}}(x)$ in (8). Moreover, the analytical methodology proposed using the CDF of $\Gamma_S^{(k,l)}$ as in (9) makes the ESR derivation of the OS scheme possible. In contrast, existing methodologies used in [2], [3], [5], [13]–[15], which are sub-optimal, consider distributions of the destination channel and eavesdropper channel separately, and hence, cannot capture the distribution of the maximal ratio of the destination to eavesdropper channel SNRs as we will do in Section III-A. The method of formulating the ESR as in (9) with the help of the CDF of $\Gamma_S^{(k,l)}$ has been explored only in [10]; however, [10] considers a different system model and a simple narrowband Rayleigh fading channel. In this paper, we face additional challenges due to the arbitrary number of destination nodes and the arbitrary number of multipath components in the destination and eavesdropper channels. In contrast, there is only one destination and one channel path in [10]. The arbitrary number of destination and multipath components makes it difficult to transform $F_{\Gamma^{(k,l)}}(x)$ into a suitable form to evaluate the integral in (9) and thus obtain a closed-form ESR solution.

Our method is also general and can be used to evaluate the ESR of more general selection schemes when the distribution of (7) and the integration in (8) are obtained in closed form. Hence, we also derive the ESR of the SS scheme, which maximizes the destination channel rate and does not consider the eavesdropping channel rate using (9), and compare it with that of the OS scheme.

On a side note, the CDF of $\Gamma_S^{(k,l)}$ can also be used to evaluate various other performance metrics such as SOP, probability of non-zero secrecy rate (PNZ), secrecy throughput [27], etc. of various node selection schemes including minimum and active eavesdropping [23], SS (system model considered in

[5], [13]-[15] and in our work), and OS.

III. ESR OF OPTIMAL SOURCE-DESTINATION PAIR SELECTION

In this section, we present the ESR analysis of the OS scheme, its high-SNR analysis, and its asymptotic limit. The OS scheme corresponds to selecting the source-destination pair for which the instantaneous secrecy rate of the system is maximized. Hence, from (7), the OS scheme satisfies

$$\Gamma_S = \max_{\forall k, \forall l} \left\{ \Gamma_S^{(k,l)} \right\} = \max_{\forall k, \forall l} \left\{ \frac{1 + \gamma_D^{(k,l)}}{1 + \gamma_E^{(k)}} \right\}$$
$$= \max_{\forall k} \left\{ \frac{1 + \max_{\forall l} \left\{ \gamma_D^{(k,l)} \right\}}{1 + \gamma_E^{(k)}} \right\}. \tag{10}$$

The ESR for the OS scheme can be evaluated via (9) with the help of the CDF of Γ_S . Thus, we proceed to find the CDF of Γ_S in the following subsection.

A. Determining the CDF of Γ_S

Our intention in this section is to find the CDF of Γ_S in a suitable form which is tractable and easily integrable in (9). By considering $\Gamma_S^{(k,l)}$ as i.i.d. random variables for all $k \in \mathcal{S}$ and $l \in \mathcal{D}$ in (7), the CDF of Γ_S is determined following the basic definition of the CDF as

$$F_{\Gamma_{S}}(x) = \mathbb{P}\left[\Gamma_{S} \leq x\right]$$

$$= \left[\int_{0}^{\infty} F_{\max\{\gamma_{D}^{(k,l)}\}}(x(1+y)-1) f_{\gamma_{E}^{(k)}}(y) dy\right]^{K}$$

$$= \left[\int_{0}^{\infty} \left(F_{\gamma_{D}^{(k,l)}}(x(1+y)-1)\right)^{L} f_{\gamma_{E}^{(k)}}(y) dy\right]^{K}$$

$$= \left[1 - \frac{1}{\lambda_{E}^{M_{E}} \Gamma(M_{E})} \sum_{l=1}^{L} (-1)^{l+1} {L \choose l} \exp\left(-\frac{l(x-1)}{\lambda_{D}}\right) \right]$$

$$\times \int_{0}^{\infty} \left(\sum_{m=0}^{M_{D}-1} \sum_{n=0}^{m} \sum_{u=0}^{m-n} (-1)^{u} {m \choose n} {m-n \choose u} \frac{x^{m-u}y^{n}}{m!\lambda_{D}^{m}}\right)^{l}$$
The great degree (16)

$$\times y^{M_E - 1} \exp\left(-\left(\frac{lx}{\lambda_D} + \frac{1}{\lambda_E}\right)y\right) dy \bigg]^K \tag{12}$$

$$= \left[1 - \Psi(x)\right]^K,\tag{13}$$

where

$$\Psi(x) = \sum_{l=1}^{L} \sum_{\mathbf{m} \in \mathcal{M}^{(l)}} \sum_{\mathbf{n} \in \mathcal{N}^{(l)}(\mathbf{m})} \sum_{\mathbf{u} \in \mathcal{U}^{(l)}(\mathbf{m}, \mathbf{n})} (-1)^{l+\widehat{u}_{p}^{(l)}+1} \binom{L}{l}
\times \frac{\lambda_{D}^{M_{E}-(\widehat{m}^{(l)}-\widehat{u}^{(l)})} \Gamma\left(M_{E}+\widehat{n}^{(l)}\right) \left(\prod_{p=1}^{l} \binom{m_{p}}{n_{p}} \binom{m_{p}-n_{p}}{u_{p}}\right)}{\lambda_{E}^{M_{E}} l^{M_{E}+\widehat{n}^{(l)}} \left(\prod_{p=1}^{l} m_{p}!\right) \Gamma(M_{E})}
\times \frac{x^{\widehat{m}^{(l)}-\widehat{u}^{(l)}} \exp\left(-\frac{l(x-1)}{\lambda_{D}}\right)}{\left(x+\frac{\lambda_{D}}{l\lambda_{E}}\right)^{M_{E}+\widehat{n}^{(l)}}}, \tag{14}$$

and using definitions

$$\widehat{m}^{(l)} \triangleq \sum_{p=1}^{l} m_p; \quad \widehat{n}^{(l)} \triangleq \sum_{p=1}^{l} n_p; \quad \widehat{u}^{(l)} \triangleq \sum_{p=1}^{l} u_p. \quad (15)$$

The expression in (13) and subsequently (14) is obtained using first the result of the form

$$\left(\sum_{i=0}^{\mu} \sum_{j=0}^{i} \sum_{v=0}^{i-j} f(i,j,v)\right)^{\zeta} \\
= \sum_{m_{1}=0}^{\mu} \sum_{n_{1}=0}^{m_{1}} \sum_{u_{1}=0}^{m_{1}-n_{1}} \dots \sum_{m_{\zeta}=0}^{\mu} \sum_{n_{\zeta}=0}^{m_{\zeta}} \prod_{v_{\zeta}=0}^{m_{\zeta}-n_{\zeta}} \prod_{p=1}^{\zeta} f(m_{p}, n_{p}, u_{p}) \\
= \sum_{\mathbf{m} \in \mathcal{M}^{(\zeta)}} \sum_{\mathbf{n} \in \mathcal{N}^{(\zeta)}(\mathbf{m})} \sum_{\mathbf{u} \in \mathcal{U}^{(\zeta)}(\mathbf{m}, \mathbf{n})} \prod_{p=1}^{\zeta} f(m_{p}, n_{p}, u_{p}), \quad (16)$$

and then with the help of an integral solution of the form [25, eq. (3.351.3)] in (12). In (16), f(i,j,v) is an arbitrary function of integers i, j and v, $\mathcal{M}^{(\zeta)}$ is the set of integer vectors $[m_1,\ldots,m_\zeta]$ containing ζ elements such that $m_p \in \{0,\ldots,\mu\}$ for each $p \in \{1,\ldots,\zeta\}$, $\mathcal{N}^{(\zeta)}(\mathbf{m})$ is the set of index vectors $[n_1,\ldots,n_\zeta]$ containing ζ elements such that $n_p \in \{0,\ldots,m_p\}$, and $\mathcal{U}^{(\zeta)}(\mathbf{m},\mathbf{u})$ is the set of integer vectors $[u_1,\ldots,u_\zeta]$ containing ζ elements such that $u_p \in \{0,\ldots,(m_p-n_p)\}$. Through binomial expansion, (13) is expressed as

$$F_{\Gamma_S}(x) = 1 - \sum_{k=1}^K (-1)^{k+1} \binom{K}{k} \Psi^k(x). \tag{17}$$

Next, we transform $\Psi^k(x)$ in (19) with the help of $\Psi(x)$ in (14) using the following result similar to (16):

$$\left(\sum_{l=1}^{L} \sum_{\mathbf{m} \in \mathcal{M}^{(l)}} \sum_{\mathbf{n} \in \mathcal{N}^{(l)}(\mathbf{m})} \sum_{\mathbf{u} \in \mathcal{U}^{(l)}(\mathbf{m}, \mathbf{n})} f(l, m_p, n_p, u_p)\right)^{k}$$

$$= \sum_{l \in \mathcal{L}^{(k)}} \sum_{\mathbf{m} \in \mathcal{M}^{(k, l)}} \sum_{\mathbf{n} \in \mathcal{N}^{(k, l)}(\mathbf{m})} \sum_{\mathbf{u} \in \mathcal{U}^{(k, l)}(\mathbf{m}, \mathbf{n})}$$

$$\left(\prod_{q=1}^{k} f(l_q, m_{q, p}, n_{q, p}, u_{q, p})\right), \tag{18}$$

where $\mathcal{L}^{(k)}$ is the set of index vectors $[l_1,\ldots,l_k]$ containing k elements such that $l_q \in \{1,\ldots,L\}$ for each $q \in \{1,\ldots,k\}$, $\mathcal{M}^{(k,1)}$ is a set of index vectors $[m_{1,1},\ldots,m_{k,l_i}]$ containing $k \times l_i$ elements such that $m_{q,p} \in \{0,\ldots,M_D-1\}$ for each $q \in \{1,\ldots,k\}$ and $p \in \{1,\ldots,l_i\}$ for each $i \in \{1,\ldots,k\}$, $\mathcal{N}^{(k,1)}(\mathbf{m})$ is the set of index vectors $[n_{1,1},\ldots,n_{k,l_i}]$ containing $k \times l_i$ elements such that $n_{q,p} \in \{0,\ldots,m_{q,p}\}$ for each $q \in \{1,\ldots,k\}$ and $p \in \{1,\ldots,l_i\}$ for each $i \in \{1,\ldots,k\}$, $\mathcal{U}^{(k,1)}(\mathbf{m},\mathbf{n})$ is the set of index vectors $[u_{1,1},\ldots,u_{k,l_i}]$ containing $k \times l_i$ elements such that $u_{q,p} \in \{0,\ldots,m_{q,p}-n_{q,p}\}$ for each $q \in \{1,\ldots,k\}$ and $p \in \{1,\ldots,k\}$ for each $i \in \{1,\ldots,k\}$ and $i \in \{1,\ldots,$

Denoting by \mathcal{X} the set of vector tuples $(\mathbf{l}, \mathbf{m}, \mathbf{n}, \mathbf{u})$ described above, $\Psi^k(x)$ in (17) can be rewritten using (18) in a form

suitable for finding the ESR, i.e.,

$$\Psi^{k}(x) = \sum_{(\mathbf{l}, \mathbf{m}, \mathbf{n}, \mathbf{u}) \in \mathcal{X}} \Upsilon \frac{x^{\widetilde{m}^{(k)} - \widetilde{u}^{(k)}} \exp(-\frac{\widetilde{l}^{(k)}}{\lambda_{D}} x)}{\prod_{q=1}^{k} \left(x + \frac{\lambda_{D}}{l_{q} \lambda_{E}}\right)^{M_{E} + \widehat{n}_{q}^{(l_{q})}}}, \quad (19)$$

where

$$\Upsilon \triangleq \prod_{q=1}^{k} (-1)^{l_q + \widehat{u}_q^{(l_q)} + 1} \binom{L}{l_q} \\
\times \frac{\lambda_D^{M_E - (\widehat{m}_q^{(l_q)} - \widehat{n}_q^{(l_q)})} \Gamma(M_E + \widehat{n}_q^{(l_q)})}{\lambda_E^{M_E} l_q^{M_E + \widehat{n}_q^{(l_q)}}} \\
\times \frac{\left(\prod_{p=1}^{l_q} \binom{m_{q,p}}{n_{q,p}} \binom{m_{q,p} - n_{q,p}}{u_{q,p}}\right) \exp\left(\frac{l_q}{\lambda_D}\right)}{\left(\prod_{p=1}^{l_q} m_{q,p}!\right) \Gamma(M_E)},$$
(20)

and

$$\widetilde{l}^{(k)} \triangleq \sum_{q=1}^{k} l_{q}; \quad \widetilde{m}^{(k)} \triangleq \sum_{q=1}^{k} \sum_{p=1}^{l_{q}} m_{q,p}; \widetilde{u}^{(k)} \triangleq \sum_{q=1}^{k} \sum_{p=1}^{l_{q}} u_{q,p}
\widehat{m}_{q}^{(l_{q})} \triangleq \sum_{p=1}^{l_{q}} m_{q,p}; \widehat{n}_{q}^{(l_{q})} \triangleq \sum_{p=1}^{l_{q}} n_{q,p}; \quad \widehat{u}_{q}^{(l_{q})} \triangleq \sum_{p=1}^{l_{q}} u_{q,p}.$$
(21)

By substituting (19) into (17) we obtain $F_{\Gamma_S}(x)$ in the form of sum-of-products which is suitable to derive the ESR using (9) in the next section.

Application of the results in (16) and (18) to convert a product of summations to a summation of products via repeated multiplications (as opposed to the method of multinomial expansion) provides a tractable approach which greatly simplifies closed-form ESR analysis. Here we note that both (16) and (18) are required due to the existence of multiple destinations, which increases the problem's difficulty level as compared to the single destination case.

B. Evaluation of ESR

The ESR is evaluated by substituting (17) in (9) as

$$C_{erg} = \frac{1}{\ln(2)} \sum_{k=1}^{K} \sum_{(\mathbf{l}, \mathbf{m}, \mathbf{n}, \mathbf{u}) \in \mathcal{X}} (-1)^{k+1} {K \choose k} \Upsilon$$

$$\times \int_{1}^{\infty} \frac{x^{\widetilde{m}^{(k)} - \widetilde{u}^{(k)} - 1} \exp(-\frac{\widetilde{l}^{(k)}}{\lambda_{D}} x)}{\prod_{q=1}^{k} \left(x + \frac{\lambda_{D}}{l_{q} \lambda_{E}}\right)^{M_{E} + \widehat{n}_{q}^{(l_{q})}} dx} \qquad (22)$$

$$= \frac{1}{\ln(2)} \sum_{k=1}^{K} \sum_{(\mathbf{l}, \mathbf{m}, \mathbf{n}, \mathbf{u}) \in \mathcal{X}} (-1)^{k+1} {K \choose k} \Upsilon$$

$$\times \left[J_{0}^{(k)} + J_{1}^{(k)} \right], \qquad (23)$$

where $J_0^{(k)}$ and $J_1^{(k)}$ correspond to the integral with $\widetilde{m}^{(k)}-\widetilde{u}^{(k)}=0$ and $\widetilde{m}^{(k)}-\widetilde{u}^{(k)}\neq 0$, respectively, and are defined

as

$$J_0^{(k)} = \int_1^\infty \frac{\exp(-\frac{\tilde{l}^{(k)}}{\lambda_D} x)}{x\left(\prod_{r=1}^k \left(x + \frac{\lambda_D}{l_q \lambda_E}\right)^{M_E + \widehat{n}_q^{(l_q)}}\right)} dx \qquad (24)$$

$$J_{1}^{(k)} = \int_{1}^{\infty} \frac{x^{\tilde{m}^{(k)} - \tilde{u}^{(k)} - 1} \exp(-\frac{\tilde{l}^{(k)}}{\lambda_{D}} x)}{\prod_{q=1}^{k} \left(x + \frac{\lambda_{D}}{l_{q} \lambda_{E}}\right)^{M_{E} + \hat{n}_{q}^{(l_{q})}} dx}.$$
 (25)

Solution of the integrals (24) and (25) are carried out in Appendix A and B, respectively. Finally the results are presented for $J_0^{(k)}$ in (26), $J_1^{(k)}$ in (27) for l_q being same for all $q \in \{1,\ldots,k\}$ in (25) , and $J_1^{(k)}$ in (28) in case any of the l_q are distinct for $q \in \{1,\ldots,k\}$ in (25). In (26)-(28), $A, B_{i,t}$ and $C_{q,t}$ are the partial fraction coefficients specific to $J_0^{(k)}$ and $J_1^{(k)}$. These and can be found for a given K, L, M_D , and M_E easily.

From the closed-form ESR presented in (23), it is difficult to interpret how the system parameters K, L, M_D , M_E , λ_D , and λ_E affect the ESR; this is due to the presence of the incomplete Gamma function as well as multiple interdependent summations. By looking at $F_{\Gamma_S}(x)$ in (17) along with (18) and (19), we observe that the ESR in (23) is also computationally intensive. As K, L and M_D (and to a lesser extent, M_E) increase, the number of summation and multiplication terms increase significantly. A more straightforward ESR expression would provide the required system design parameters quickly when the system is optimized with this metric. Simplified system design is preferable in online systems where latency is a limiting factor, such as delay-sensitive communications in IoT applications. Hence, in the following two sections, we analyze the ESR in the high-SNR regime, and we also find the asymptotic ESR using a less complex expression which can provide further insight.

Next, we provide the result for the special case of a single destination.

1) Single Destination Case: For a special case of L=1, (23) is obtained as

$$C_{erg} = \frac{1}{\ln(2)} \sum_{k=1}^{K} (-1)^{k+1} {K \choose k} \left[I_0^{(k)} + I_1^{(k)} \right], \tag{29}$$

where $I_0^{(k)}$ corresponds to the case where $\widehat{n}^{(k)}+u=0$, and is expressed as

$$I_{0}^{(k)} = \sum_{\mathbf{m} \in \mathcal{M}^{(k)}} (-1)^{\widehat{m}^{(k)}} \frac{\lambda_{D}^{kM_{E} - \widehat{m}^{(k)}} \exp\left(\frac{k}{\lambda_{D}}\right)}{\lambda_{E}^{kM_{E}} \left(\prod_{q=1}^{k} m_{q}!\right)} \times \left[\Gamma\left(0, \frac{k}{\lambda_{D}}\right) - \exp\left(\frac{k}{\lambda_{E}}\right) \sum_{t=1}^{kM_{E}} \left(\frac{k}{\lambda_{E}}\right)^{kM_{E} - t} \times \Gamma\left(-\left(kM_{E} - t\right), \frac{k}{\lambda_{D}} \left(1 + \frac{\lambda_{D}}{\lambda_{E}}\right)\right)\right]. \tag{30}$$

Similarly, $I_1^{(k)}$ corresponds to the condition $\widehat{n}^{(k)}+u\neq 0$, and is expressed as

$$I_{1}^{(k)} = \sum_{\mathbf{m} \in \mathcal{M}^{(k)}} \sum_{\mathbf{n} \in \mathcal{N}(\mathbf{m})} \sum_{u=0}^{\widehat{m}^{(k)} - \widehat{n}^{(k)}} \sum_{j=0}^{\widehat{n}^{(k)} + u - 1} (-1)^{\widehat{m}^{(k)} + \widehat{n}^{(k)} + u + j}$$

$$\times \frac{\left(\widehat{m}^{(k)} - \widehat{n}^{(k)}\right) \left(\widehat{n}^{(k)} + u - 1\right) \left(\prod_{q=1}^{k} \binom{m_q}{n_q} \Gamma\left(M_E + n_q\right)\right)}{k^{u - kM_E - j} \lambda_D^{\widehat{m}^{(k)} - \widehat{n}^{(k)} - u} \lambda_E^{kM_E + j} \left(\prod_{q=1}^{k} m_q!\right) \Gamma(M_E)^k}$$

$$\times \Gamma\left(-\left(kM_E - u + j\right), \frac{k}{\lambda_D} \left(1 + \frac{\lambda_D}{\lambda_E}\right)\right) \exp\left(\frac{k}{\lambda_D} + \frac{k}{\lambda_E}\right)$$
(31)

Thus, when L=1, partial fraction coefficients are available in closed form, and by employing those coefficients the exact ESR is expressed in (29) which is much simpler than the corresponding expression (23) for multiple destination case.

C. High-SNR Approximation

To reduce the computational complexity of the solution and to assess more easily the behavior of the ESR with the system parameters K, L, M_D , M_E , λ_D , and λ_E , in this subsection, we determine an approximate ESR expression at high SNR. This high-SNR approximation also helps us find the asymptotic ESR in the next section.

By the "high-SNR" condition, we mean that $\gamma_D^{(k,l)} >> 1$ and $\gamma_E^{(k)} >> 1$ for all k and l. Therefore, we use the approximation $\Gamma_S^{(k,l)} = \frac{1+\max\limits_{\forall l}\left\{\gamma_D^{(k,l)}\right\}}{1+\gamma_E^{(k)}} \approx \frac{\max\limits_{\forall l}\left\{\gamma_D^{(k,l)}\right\}}{\gamma_E^{(k)}}$ in (10). With this approximation, the high-SNR CDF of Γ_S in (11) is then obtained as

$$F_{\Gamma_S}(x) = \mathbb{P}\left[\Gamma_S \le x\right]$$

$$= \left[\int_0^\infty F_{\max\{\gamma_D^{(k,l)}\}}(xy) f_{\gamma_E^{(k)}}(y) dy\right]^K. \tag{32}$$

The integral solution above is expressed exactly as in (17), where

$$\Psi(x) = \sum_{l=1}^{L} \sum_{\mathbf{m} \in \mathcal{M}^{(l)}} (-1)^{l+1} \binom{L}{l}$$

$$\times \frac{\lambda_D^{M_E} \Gamma\left(M_E + \widehat{m}^{(l)}\right) x^{\widehat{m}^{(l)}}}{\lambda_E^{M_E} l^{M_E} + \widehat{m}^{(l)} \left(\prod_{p=1}^{l} m_p!\right) \Gamma(M_E) \left(x + \frac{\lambda_D}{l\lambda_E}\right)^{M_E + \widehat{m}^{(l)}}}.$$
(33)

This expression is obtained using manipulations similar to those used in the derivation of (14) in the exact ESR analysis. As we did in (19), we convert $\Psi^k(x)$ from a product-of-sums into a sum-of-products form to evaluate the ESR, yielding

$$\Psi^{k}(x) = \sum_{\mathbf{l} \in \mathcal{L}^{(k)}} \sum_{\mathbf{m} \in \mathcal{M}^{(k,l_{k})}} \Upsilon \frac{x^{\widetilde{m}^{(k)}}}{\prod\limits_{q=1}^{k} \left(x + \frac{\lambda_{D}}{l_{q}\lambda_{E}}\right)^{M_{E} + \widehat{m}_{q}^{(l_{q})}}}, \quad (34)$$

$$J_{0}^{(k)} = A\Gamma\left(0, \frac{\widetilde{l}^{(k)}}{\lambda_{D}}\right) + \sum_{i=1}^{\mathcal{I}} \sum_{t=1|q \in \mathcal{Q}_{i}}^{\sum_{l=1}|\widetilde{q}_{q} \in \mathcal{Q}_{i}} B_{i,t}\left(\frac{\widetilde{l}^{(k)}}{\lambda_{D}}\right)^{t-1} \exp\left(\frac{\widetilde{l}^{(k)}}{l_{q}\lambda_{E}}\right) \Gamma\left(-t+1, \frac{\widetilde{l}^{(k)}}{\lambda_{D}}\left(1+\frac{\lambda_{D}}{\lambda_{D}}\right)\right)$$

$$+ \sum_{q \in \mathcal{Q}} \sum_{t=1}^{M_{E} + \widetilde{\Omega}_{q}^{(l_{q})}} C_{q,t}\left(\frac{\widetilde{l}^{(k)}}{\lambda_{D}}\right)^{t-1} \exp\left(\frac{\widetilde{l}^{(k)}}{l_{q}\lambda_{E}}\right) \Gamma\left(-t+1, \frac{\widetilde{l}^{(k)}}{\lambda_{D}}\left(1+\frac{\lambda_{D}}{l_{q}\lambda_{E}}\right)\right). \tag{26}$$

$$J_{1}^{(k)} = \sum_{j=0}^{\widetilde{m}^{k} - \widetilde{u}^{k} - 1} \left(\widetilde{m}^{k} - \widetilde{u}^{k} - 1\right) \left(-\frac{\lambda_{D}}{l_{q}\lambda_{E}}\right)^{\widetilde{m}^{k} - \widetilde{u}^{k} - 1 - j} \exp\left(\frac{\widetilde{l}^{(k)}}{l_{q}\lambda_{E}}\right)$$

$$\times \left(\frac{\widetilde{l}^{(k)}}{\lambda_{D}}\right)^{-(j-kM_{E} - \sum_{q=1}^{k} \widetilde{n}_{q}^{(l_{q})}) - 1} \Gamma\left(j - kM_{E} - \sum_{q=1}^{k} \widehat{n}_{q}^{(l_{q})} + 1, \frac{\widetilde{l}^{(k)}}{\lambda_{D}}\left(1 + \frac{\lambda_{D}}{l_{q}\lambda_{E}}\right)\right). \tag{27}$$

$$J_{1}^{(k)} = \sum_{i=1}^{\mathcal{I}} \sum_{t=1|q \in \mathcal{Q}_{i}} \sum_{j=0}^{\widetilde{n}_{q}^{(l_{q})}} \widetilde{m}^{k} - \widetilde{u}^{k} - 1 \exp\left(\frac{\widetilde{l}^{(k)}}{l_{q}\lambda_{E}}\right) \left(\widetilde{m}^{k} - \widetilde{u}^{k} - 1\right) \left(-\frac{\lambda_{D}}{l_{q}\lambda_{E}}\right)^{\widetilde{m}^{k} - \widetilde{u}^{k} - 1 - j} B_{i,t}$$

$$\times \left(\frac{\widetilde{l}^{(k)}}{\lambda_{D}}\right)^{-(j-t)-1} \Gamma\left(j - t + 1, \frac{\widetilde{l}^{(k)}}{\lambda_{D}}\left(1 + \frac{\lambda_{D}}{l_{q}\lambda_{E}}\right)\right)$$

$$+ \sum_{q \in \mathcal{Q}} \sum_{t=1}^{M_{E} + \widetilde{n}_{q}^{(l_{q})}} \widetilde{m}^{k} - \widetilde{u}^{k} - 1} \exp\left(\frac{\widetilde{l}^{(k)}}{l_{q}\lambda_{E}}\right) \left(\widetilde{m}^{k} - \widetilde{u}^{k} - 1\right) \left(-\frac{\lambda_{D}}{l_{q}\lambda_{E}}\right)^{\widetilde{m}^{k} - \widetilde{u}^{k} - 1 - j} C_{q,t}$$

$$\times \left(\frac{\widetilde{l}^{(k)}}{\lambda_{D}}\right)^{-(j-t)-1} \Gamma\left(j - t + 1, \frac{\widetilde{l}^{(k)}}{l_{q}\lambda_{E}}\right) \left(\widetilde{m}^{k} - \widetilde{u}^{k} - 1\right). \tag{28}$$

where

$$\Upsilon \triangleq \prod_{q=1}^{k} (-1)^{l_q+1} \binom{L}{l_q} \frac{\lambda_D^{M_E} \Gamma\left(M_E + \widehat{m}_q^{(l_q)}\right)}{\lambda_E^{M_E} l_q^{M_E + \widehat{m}_q^{(l_q)}} \left(\prod_{p=1}^{l_q} m_{q,p}!\right) \Gamma(M_E)}$$
(35)

with the definitions already provided in (21). By substituting (34) in (17) and then using (9), the ESR in (22) becomes, at high SNR,

$$C_{erg} = \frac{1}{\ln(2)} \sum_{k=1}^{K} \sum_{\mathbf{l} \in \mathcal{L}^{(k)}} \sum_{\mathbf{m} \in \mathcal{M}^{(k,\mathbf{l})}} (-1)^{k+1} {K \choose k} \Upsilon \times \left[J_0^{(k)} + J_1^{(k)} \right].$$
 (36)

Similar to (23), $J_0^{(k)}$ corresponds to the case when $\widetilde{m}^{(k)}=0$ and $J_1^{(k)}$ corresponds to the case when $\widetilde{m}^{(k)}\neq 0$. $J_0^{(k)}$ and $J_1^{(k)}$ are expressed as

$$J_0^{(k)} = \int_1^\infty \frac{1}{x \left(\prod_{q=1}^k \left(x + \frac{\lambda_D}{l_q \lambda_E}\right)^{M_E}\right)} dx \tag{37}$$

$$J_1^{(k)} = \int_1^\infty \frac{x^{\widetilde{m}^{(k)} - 1}}{\prod_{q=1}^k \left(x + \frac{\lambda_D}{l_q \lambda_E} \right)^{M_E + \widehat{m}_q^{(l_q)}}} dx.$$
 (38)

The solution approach of $J_0^{(k)}$ at high SNR in (37) is similar to that of $J_0^{(k)}$ in (81) following the partial fraction method. The solution is presented in (39). The solution of the integral (38) is

presented in Appendix C. An expression for $J_1^{(k)}$ is presented in (40) for the case where l_q are equal for all $q \in \{1, \ldots, k\}$, $\Upsilon \triangleq \prod_{q=1}^k (-1)^{l_q+1} \binom{L}{l_q} \frac{\lambda_D^{M_E} \Gamma\left(M_E + \widehat{m}_q^{(l_q)}\right)}{\lambda_E^{M_E} l_q^{M_E + \widehat{m}_q^{(l_q)}} \left(\prod_{p=1}^{l_q} m_{q,p}!\right) \Gamma(M_E)}, \quad \text{and in (41) for the case where any of the } l_q \text{ are unequal for } q \in \{1, \dots, k\} \text{ in (38)}. \\ B_{i,t} \text{ and } C_{q,t} \text{ are the partial fraction coefficients specific to } J_0^{(k)} \text{ and } J_1^{(k)} \text{ at high SNR and can be } I_q = I_q + I_q +$ easily obtained for a given K, L, M_D , and M_E .

> By comparing the exact ESR in (23) and the high-SNR approximate ESR in (36), we observe that evaluating the exact ESR is more computationally intensive than the high-SNR ESR as the summations over $\mathcal{N}^{(k,\mathbf{l})}(\mathbf{m})$ and $\mathcal{U}^{(k,\mathbf{l})}(\mathbf{m},\mathbf{n})$ are absent in (22). To understand the complexity advantage of computation in the high-SNR regime more precisely and to obtain insights, we focus in the following on the special case of a single destination.

> 1) High-SNR Approximation in Single Destination Case: For the special case of L = 1, (36) has the form of (29), where

$$I_0^{(k)} = \ln\left(1 + \frac{\lambda_D}{\lambda_E}\right) - \sum_{t=1}^{kM_E - 1} \frac{\left(\frac{\lambda_D}{\lambda_E}\right)^{kM_E - t}}{\left(1 + \frac{\lambda_D}{\lambda_E}\right)^{kM_E - t} (kM_E - t)}, \tag{42}$$

$$I_1^{(k)} = \sum_{\mathbf{m} \in \mathcal{M}^{(k)}} \sum_{j=0}^{\widehat{m}^{(k)} - 1} (-1)^{\widehat{m}^{(k)} - j - 1} {\widehat{m}^{(k)} - 1 \choose j}$$

$$J_{0}^{(k)} = \sum_{i=1}^{\mathcal{I}} \sum_{t=1|q \in \mathcal{Q}_{i}}^{1} B_{i,t} \ln\left(1 + \frac{\lambda_{D}}{l_{q}\lambda_{E}}\right) + \sum_{i=1}^{\mathcal{I}} \sum_{t=2|q \in \mathcal{Q}_{i}}^{|\mathcal{Q}_{i}|M_{E}} \frac{B_{i,t}}{(t-1)\left(1 + \frac{\lambda_{D}}{l_{q}\lambda_{E}}\right)^{t-1}} + \sum_{q \in \mathcal{Q}} \sum_{t=1}^{1} C_{q,t} \ln\left(1 + \frac{\lambda_{D}}{l_{q}\lambda_{E}}\right) + \sum_{q \in \mathcal{Q}} \sum_{t=2}^{M_{E}} \frac{C_{q,t}}{(t-1)\left(1 + \frac{\lambda_{D}}{l_{q}\lambda_{E}}\right)^{t-1}}.$$
(39)

$$J_1^{(k)} = \sum_{j=0}^{\widetilde{m}^{(k)}-1} {\widetilde{m}^{(k)}-1 \choose j} \left(-\frac{\lambda_D}{l_q \lambda_E}\right)^{\widetilde{m}^{(k)}-1-j} \frac{\left(1+\frac{\lambda_D}{l_q \lambda_E}\right)^{-(kM_E+\widetilde{m}^{(k)}-1-j)}}{kM_E+\widetilde{m}^{(k)}-1-j}.$$
 (40)

$$J_{1}^{(k)} = \sum_{i=1}^{\mathcal{I}} \sum_{t=1}^{1} -B_{i,t} \ln\left(1 + \frac{\lambda_{D}}{l_{q}\lambda_{E}}\right) + \sum_{i=1}^{\mathcal{I}} \sum_{t=2|q \in \mathcal{Q}_{i}}^{|\mathcal{Q}_{i}|M_{E} + \sum_{q \in \mathcal{Q}_{i}} \widehat{m}_{q}^{l_{q}}} \frac{B_{i,t}}{(t-1)\left(1 + \frac{\lambda_{D}}{l_{q}\lambda_{E}}\right)^{t-1}} + \sum_{q \in \bar{\mathcal{Q}}} \sum_{t=1}^{1} -C_{q,t} \ln\left(1 + \frac{\lambda_{D}}{l_{q}\lambda_{E}}\right) + \sum_{q \in \bar{\mathcal{Q}}} \sum_{t=2}^{M_{E} + \widehat{m}_{q}^{l_{q}}} \frac{C_{q,t}}{(t-1)\left(1 + \frac{\lambda_{D}}{l_{q}\lambda_{E}}\right)^{t-1}}.$$

$$(41)$$

$$\times \frac{\left(\frac{\lambda_{D}}{\lambda_{E}}\right)^{(kM_{E}+\widehat{m}^{(k)}-j-1)} \left(\prod_{q=1}^{k} \Gamma\left(M_{E}+m_{q}\right)\right)}{\left(1+\frac{\lambda_{D}}{\lambda_{E}}\right)^{\left(kM_{E}+\widehat{m}^{(k)}-j-1\right)} \left(\prod_{q=1}^{k} m_{q}!\right) \Gamma(M_{E})^{k}} \times \frac{1}{\left(kM_{E}+\widehat{m}^{(k)}-j-1\right)}.$$
(43)

We notice that the ESR in (23) with high-SNR approximation via (42) and (43) is a summation of two components. One component varies as a logarithmic function of the ratio λ_D/λ_E and is independent of K, M_D , and M_E , the other component tends to a constant as λ_D/λ_E grows asymptotically; however, it depends on K, M_D , and M_E . This will be made clearer when we present the asymptotic analysis in the next section.

If we compare the computational complexity in terms of the number of addition and multiplication operations required to compute the exact ESR for the single destination case, it can be seen that the high-SNR approximate expression is less computationally intensive. This is due to the fact that the CDF of $\Gamma_S^{(k)}$ in (17) has a smaller number of summation terms in the high-SNR approximation scenario. For L=1, the computation of the CDF in (17) for the exact ESR using $\Psi^k(x)$ in (14) with the help of (16) requires $\sum_{k=1}^K (M_D(M_D+1)/2)^k$ additions, which is in the order of $\sum_{k=1}^K (M_D/\sqrt{2})^{2k} \approx (M_D/\sqrt{2})^{2K}$. For the k^{th} summation iteration, there are k multiplications, therefore the number of multiplications required is in the order of $\sum_{k=1}^K (k(M_D/\sqrt{2})^{2k}) \approx (K(M_D/\sqrt{2})^{2K})$. The computation of the CDF in (17) for the high-SNR approximation using $\Psi^k(x)$ in (34) requires $\sum_{k=1}^K M_D^k$ additions. Hence, it is in the order of M_D^K . Also, as k multiplications are required in the k^{th} summation iteration, the number of multiplications is in the order of KM_D^K . Clearly, the high-SNR approximation has lower computational complexity.

D. Asymptotic Analysis

To provide better insight regarding how the ESR depends on the system parameters K, L, M_D , M_E , λ_D , and λ_E , we perform asymptotic analysis by assuming $\lambda_D \to \infty$ for a given

 λ_E in the high-SNR approximate ESR expression derived in (36). This assumption is based on a practical scenario where the destinations are closer to the transmitters than the eavesdropper. With this assumption, using the approximation $1 + \frac{\lambda_D}{l_q \lambda_E} \approx \frac{\lambda_D}{l_q \lambda_E}$ for each $q \in \{1, \dots, k\}$ in $J_0^{(k)}$ given by (43) (39) we find

$$J_0^{(k)} = \sum_{i=1}^{\mathcal{I}} \sum_{t=1|q \in \mathcal{Q}_i}^{1} B_{i,t} \ln\left(\frac{\lambda_D}{l_q \lambda_E}\right)$$

$$+ \sum_{i=1}^{\mathcal{I}} \sum_{t=2|q \in \mathcal{Q}_i}^{|\mathcal{Q}_i| M_E} \frac{B_{i,t}}{(t-1)\left(\frac{\lambda_D}{l_q \lambda_E}\right)^{t-1}}$$

$$+ \sum_{q \in \bar{\mathcal{Q}}} \sum_{t=1}^{1} C_{q,t} \ln\left(\frac{\lambda_D}{l_q \lambda_E}\right)$$

$$+ \sum_{q \in \bar{\mathcal{Q}}} \sum_{t=2}^{M_E} \frac{C_{q,t}}{(t-1)\left(\frac{\lambda_D}{l_q \lambda_E}\right)^{t-1}}.$$
(44)

Using the same approximation in (84), we obtain $J_1^{(k)}$ when all l_q are equal for all $q \in \{1, \ldots, k\}$ as

$$J_{1}^{(k)} = \sum_{j=0}^{\widetilde{m}^{(k)}-1} (-1)^{\widetilde{m}^{(k)}-1-j} {\widetilde{m}^{(k)}-1 \choose j} \times \frac{\left(\frac{\lambda_{D}}{l_{q}\lambda_{E}}\right)^{-kM_{E}}}{kM_{E} + \widetilde{m}^{(k)} - 1 - j}, \tag{45}$$

and when any of the l_q are unequal for $q \in \{1, \dots, k\}$ in (85) as

$$J_1^{(k)} = \sum_{i=1}^{\mathcal{I}} \sum_{t=1}^{1} -B_{i,t} \ln \left(\frac{\lambda_D}{l_q \lambda_E} \right)$$

$$+ \sum_{i=1}^{\mathcal{I}} \sum_{t=2|q \in \mathcal{Q}_i}^{|\mathcal{Q}_i| M_E + \sum_{q \in \mathcal{Q}_i} \widehat{m}_q^{l_q}} \frac{B_{i,t}}{(t-1) \left(\frac{\lambda_D}{l_q \lambda_E} \right)^{t-1}}$$

$$+ \sum_{q \in \bar{\mathcal{Q}}} \sum_{t=1}^{1} -C_{q,t} \ln \left(\frac{\lambda_D}{l_q \lambda_E} \right)$$

$$+\sum_{q\in\bar{Q}}\sum_{t=2}^{M_E+\hat{m}_q^{l_q}}\frac{C_{q,t}}{(t-1)(\frac{\lambda_D}{l_q\lambda_E})^{t-1}}.$$
 (46)

The asymptotic ESR C_{erg}^{∞} is obtained by substituting (44), (45) and (46) into (36). Next, we analyze the special case of a single destination for more insights.

1) Asymptotic Analysis in Single Destination Case: By substituting $1 + \frac{\lambda_D}{\lambda_E} \approx \frac{\lambda_D}{\lambda_E}$ in (42) and after performing some mathematical simplifications, we find

$$I_0^{(k)} = \ln\left(\frac{\lambda_D}{\lambda_E}\right) - \sum_{i=1}^{kM_E - 1} \frac{1}{kM_E - i}$$
$$= \ln\left(\frac{\lambda_D}{\lambda_E}\right) - H_{kM_E - 1}, \tag{47}$$

where H_N is the N^{th} harmonic number. Using the same approximation in (43), and after writing $\binom{\widehat{m}^{(k)}-1}{j}$ in the factorial form, we obtain $I_1^{(k)}$ as

$$I_{1}^{(k)} = \sum_{\mathbf{m} \in \mathcal{M}^{(k)}} \frac{\left(\prod_{q=1}^{k} \Gamma\left(M_{E} + m_{q}\right)\right)}{\left(\prod_{q=1}^{k} m_{q}!\right) \Gamma(M_{E})^{k}} \times \sum_{u=0}^{\widehat{m}^{(k)} - 1} \frac{(-1)^{\widehat{m}^{(k)} - u - 1} \Gamma(\widehat{m}^{(k)})}{u!(\widehat{m}^{(k)} - u - 1)! \left(kM_{E} + \widehat{m}^{(k)} - u - 1\right)}$$
(48)
$$= \sum_{\mathbf{m} \in \mathcal{M}^{(k)}} \frac{\left(\prod_{q=1}^{k} \Gamma\left(M_{E} + m_{q}\right)\right) \Gamma(\widehat{m}^{(k)})(kM_{E} - 1)!}{\left(\prod_{q=1}^{k} m_{q}!\right) \Gamma(M_{E})^{k}(kM_{E} + \widehat{m}^{(k)} - 1)!} \Xi,$$
(49)

where

$$\Xi = \sum_{v=0}^{\widehat{m}^{(k)}-1} (-1)^{\widehat{m}^{(k)}-v-1} \times \frac{\prod_{u=0, u\neq v}^{\widehat{m}^{(k)}-1} \left(u!(\widehat{m}^{(k)}-u-1)!(kM_E + \widehat{m}^{(k)}-u-1) \right)}{\prod_{u=0}^{\widehat{m}^{(k)}-1} \left(u!(\widehat{m}^{(k)}-u-1)! \right)} = 1.$$
(50)

The expression (49) above is obtained after multiplying both the numerator and denominator of (48) by $(kM_E-1)!$ and performing some mathematical simplifications. The proof that $\Xi=1$ is straightforward and is omitted due to space constraints.

The asymptotic ESR, C_{erg}^{∞} , is obtained by substituting (47) and (49) into (23). After a few simplifications, C_{erg}^{∞} is expressed as

$$C_{\text{erg}}^{\infty} = \log_2\left(\frac{\lambda_D}{\lambda_E}\right) - \frac{1}{\ln(2)} \sum_{k=1}^K (-1)^{k+1} {K \choose k} \psi_{\infty}^{(k)},$$
 (51)

where

$$\psi_{\infty}^{(k)} = H_{kM_E - 1} - I_1^{(k)}. (52)$$

From (47) and (49), it is clear that the asymptotic ESR depends on the ratio λ_D/λ_E . This ratio arises in the expression for $I_0^{(k)}$; however, $I_1^{(k)}$ is independent of the ratio. This shows that one part of the ESR varies linearly with the ratio λ_D/λ_E in the logarithmic scale, while the other part is independent of this ratio. As the ratio λ_D/λ_E increases asymptotically, (51) becomes independent of all system parameters except this ratio. We now express the asymptotic ESR as a linear function of $\log_2(\lambda_D)$ as (c.f. [10], [28]),

$$C_{\text{erg}}^{\infty} = \mathcal{S}_{\infty} \left(\log_2 \left(\lambda_D \right) - \mathcal{L}_{\infty} \right), \tag{53}$$

where S_{∞} is the slope, i.e., the maximum multiplexing gain or number of degrees of freedom, and \mathcal{L}_{∞} is the high-SNR offset. By observing (51), the slope and high-SNR offset are given by

$$\mathcal{S}_{\infty} = 1$$
, and
$$\mathcal{L}_{\infty} = \log_2(\lambda_E) + \frac{1}{\ln(2)} \sum_{k=1}^K (-1)^{k+1} {K \choose k} \psi_{\infty}^{(k)}, \quad (54)$$

respectively.

We conclude from (53) and (54) in the high-SNR regime, the ESR varies linearly with λ_D in the logarithmic scale. The high-SNR slope is always unity and does not depend on K, M_D , or M_E . On the other hand, the high-SNR offset is independent of λ_D and depends on λ_E , M_E , M_D , and K. We can also easily identify from (54) that as λ_E increases, the high-SNR offset increases, and as a result the ESR decreases.

When K > 1 and $M_D = M_E$, we see from (52) that the high-SNR offset varies with M_D . This means that the number of multipath components has a significant effect on the ESR performance of the OS scheme. However, as a reference we note that in the special case when K = 1 and $M_D = M_E$, we have $\psi_{\infty}^{(1)} = 0$, since

$$\psi_{\infty}^{(1)} = H_{M_E - 1} - H_{M_D - 1},\tag{55}$$

due to $I_1^{(1)} = \sum_{m_1=1}^{M_D-1} \frac{1}{m_1} = H_{M_D-1}$ in (49). Hence, the offset $\mathcal{L}_{\infty} = \log_2{(\lambda_E)}$ is the same as the offset under Rayleigh fading channel conditions, i.e., $M_D = M_E = 1$. This means for a single-transmitter system with an arbitrary but equal number of multipath components in the destination and eavesdropper channels, the ESR will asymptotically approach the narrowband Rayleigh fading channel ESR.

For the case of Rayleigh fading channels, i.e., $M_D = M_E = 1$, with arbitrary K, from (52) we have $\psi_{\infty}^{(k)} = H_{k-1}$ as $I_1^{(k)}$ exists only for $\widehat{m}^{(k)} \neq 0$. Hence, from (54), the slope is $\mathcal{S}_{\infty} = 1$ and the offset is

$$\mathcal{L}_{\infty} = \log_2(\lambda_E) - \frac{1}{\ln(2)} \sum_{k=1}^K (-1)^k {K \choose k} H_{k-1}$$
$$= \log_2(\lambda_E) - \frac{1}{\ln(2)} H_{K-1}. \tag{56}$$

This special case expression for the ESR exactly matches the ESR expression derived in [10] for the OS scheme with unreliable backhaul and multiple eavesdroppers in Rayleigh fading when backhaul is considered to be perfect and there is a single eavesdropper.

IV. ESR OF SUB-OPTIMAL SOURCE-DESTINATION PAIR SELECTION

The SS scheme is implemented when the CSI of the link S_k -E is not available for any $k \in \mathcal{S}$. In this scenario, the source-destination pair is selected for which $\gamma_D^{(k,l)}$ is maximum among all k and l. In this scheme, Γ_S is written as

$$\Gamma_S = \frac{1 + \max_{\forall k, \forall l} \left\{ \gamma_D^{(k,l)} \right\}}{1 + \gamma_E^{(k^*)}},\tag{57}$$

where $\gamma_E^{(k^*)}$ is the SNR at E corresponding to the selected transmitter k^* . As S_k -E for each k is i.i.d., $\gamma_E^{(k^*)}$ follows the distribution expressed in (5). In Section III, we proposed a way to evaluate the ESR of the OS scheme; in this section we will show that it can also be extended for the SS scheme. We first proceed with the evaluation of the CDF of Γ_S .

A. Determining the CDF of Γ_S

As $\Gamma_S^{(k,l)}$ for all $k\in\mathcal{S}$ and $l\in\mathcal{D}$ is i.i.d., the CDF of Γ_S is derived as

$$F_{\Gamma_{S}}(x) = \mathbb{P}\left[\max_{\forall k, \forall l} \left\{\gamma_{D}^{(k,l)}\right\} \le x \left(1 + \gamma_{E}^{(k^{*})}\right) - 1\right]$$

$$= \int_{0}^{\infty} \left[F_{\gamma_{D}^{(k,l)}}(x(1+y) - 1)\right]^{KL} f_{\gamma_{E}^{(k^{*})}}(y) \, dy$$
(58)

where

$$\Psi^{k}(x) = \int_{0}^{\infty} \Psi^{k}(x, y) f_{\gamma_{E}^{(k^{*})}}(y) dy$$
 (59)

and

$$\Psi^{k}(x,y) = \left[\sum_{m=0}^{M_{D}-1} \sum_{n=0}^{m} {m \choose n} \frac{(x-1)^{m-n} x^{n} y^{n} \exp\left(-\frac{x(1+y)-1}{\lambda_{D}}\right)}{(m!) \lambda_{D}^{m}} \right]^{k}$$

$$= \sum_{\mathbf{m} \in \mathcal{M}^{(k)}} \sum_{\mathbf{n} \in \mathcal{N}^{(k)}(\mathbf{m})} \sum_{j=0}^{\widehat{m}^{(k)} - \widehat{n}^{(k)}} (-1)^{\widehat{m}^{(k)} - \widehat{n}^{(k)} - j}$$

$$\times \left(\widehat{m}^{(k)} - \widehat{n}^{(k)} \right) \frac{\left(\prod_{q=1}^{k} {m_{q} \choose n_{q}} \right) x^{\widehat{n}^{(k)} + j} \exp\left(-\frac{k(x-1)}{\lambda_{D}}\right)}{\left(\prod_{q=1}^{k} m_{q}! \right) \lambda_{D}^{\widehat{m}^{(k)}}}$$

$$\times y^{\widehat{n}^{(k)}} \exp\left(-\frac{kxy}{\lambda_{D}}\right). \tag{60}$$

The derivation of $\Psi^k(x,y)$ in (60) using (16) is similar to the method adopted in the OS scheme. Then, the solution of the integral in (59) is obtained with the help of [25, eq. (3.351.3)] as

$$\Psi^{k}(x) = \sum_{\mathbf{m} \in \mathcal{M}^{(k)}} \sum_{\mathbf{n} \in \mathcal{N}^{(k)}(\mathbf{m})} \sum_{j=0}^{\widehat{m}^{(k)} - \widehat{n}^{(k)}} (-1)^{\widehat{m}^{(k)} - \widehat{n}^{(k)} - j} \times {\widehat{m}^{(k)} - \widehat{n}^{(k)} \choose j} \frac{\lambda_{D}^{M_{E} - (\widehat{m}^{(k)} - \widehat{n}^{(k)})} \Gamma(M_{E} + \widehat{n}^{(k)})}{\lambda_{E}^{M_{E}} k^{M_{E} + \widehat{n}^{(k)}} \left(\prod_{q=1}^{k} m_{q}!\right) \Gamma(M_{E})}$$

$$\times \frac{\left(\prod_{q=1}^{k} {m_q \choose n_q}\right) x^{\widehat{n}^{(k)}+j} \exp\left(-\frac{k(x-1)}{\lambda_D}\right)}{\left(x + \frac{\lambda_D}{k\lambda_E}\right)^{M_E + \widehat{n}^{(k)}}}.$$
 (61)

B. Evaluation of ESR

Substituting (61) into (9), the ESR in SS can be expressed as

$$C_{erg} = \frac{1}{\ln(2)} \sum_{k=1}^{KL} (-1)^{k+1} {KL \choose k} \int_{1}^{\infty} \frac{\Psi^{k}(x)}{x} dx$$
$$= \frac{1}{\ln(2)} \sum_{k=1}^{KL} (-1)^{k+1} {KL \choose k} \left[I_{0}^{(k)} + I_{1}^{(k)} \right], \qquad (62)$$

where I_0 corresponds to the integral with condition $\hat{n}^{(k)} + j = 0$ and is expressed as

$$I_0^{(k)} = \sum_{\mathbf{m} \in \mathcal{M}^{(k)}} (-1)^{\widehat{m}^{(k)}} \frac{\lambda_D^{M_E}}{\lambda_D^{\widehat{m}^{(k)}} k^{M_E} \lambda_E^{M_E} \left(\prod_{q=1}^k m_q!\right)} \times \int_1^\infty \frac{\exp\left(-\frac{k(x-1)}{\lambda_D}\right)}{x \left(x + \frac{\lambda_D}{k\lambda_E}\right)^{M_E}} dx, \tag{63}$$

and I_1 correspond to the integral with condition $\widehat{n}^{(k)}+j>0$ and is expressed as

$$I_{1}^{(k)} = \sum_{\mathbf{m} \in \mathcal{M}^{(k)}} \sum_{\mathbf{n} \in \mathcal{N}^{(k)}(\mathbf{m})} \sum_{j=0}^{\widehat{m}^{(k)} - \widehat{n}^{(k)}} (-1)^{\widehat{m}^{(k)} - \widehat{n}^{(k)} - j}$$

$$\times \left(\widehat{m}^{(k)} - \widehat{n}^{(k)} \right) \frac{\lambda_{D}^{M_{E} - (\widehat{m}^{(k)} - \widehat{n}^{(k)})} \Gamma(M_{E} + \widehat{n}^{(k)})}{\lambda_{E}^{M_{E}} k^{M_{E} + \widehat{n}^{(k)}} \left(\prod_{q=1}^{k} m_{q}! \right) \Gamma(M_{E})}$$

$$\times \int_{1}^{\infty} \frac{\left(\prod_{q=1}^{k} \binom{m_{q}}{n_{q}} \right) x^{\widehat{n}^{(k)} + j - 1} \exp\left(- \frac{k(x-1)}{\lambda_{D}} \right)}{(x + \frac{\lambda_{D}}{\lambda_{D}})^{M_{E} + \widehat{n}^{(k)}}} dx. \quad (64)$$

The solutions of $I_0^{(k)}$ and $I_1^{(k)}$ are provided into (65) and (66) respectively. With the substitution of (65) and (66) in (62), the ESR is expressed in closed form. Here we note that in (62) if the total number of links KL is the same for any combination of K and L, the ESR performance would be the same for these combinations. Thus increasing either K or L is identical for the system secrecy in the SS scheme.

From (62) it is difficult to gain insights. Hence, we provide a high-SNR approximation and asymptotic analysis in the following sections, as was provided for the OS scheme in Sections III-C and III-D, respectively.

C. High-SNR Approximation

In the high-SNR regime, as in the OS scheme, we assume $\max_{\forall k, \forall l} \{\gamma_D^{(k,l)}\} >> 1$ and $\gamma_E^{(k^*)} >> 1$ for all k and l, thus we use

the approximation $\Gamma_S^{(k,l)} \approx \frac{\max\limits_{\forall k,\forall l} \{\gamma_D^{(k,l)}\}}{\gamma_E^{(k^*)}}$ by neglecting unity from the numerator and denominator in (57). As discussed in the OS scheme, this forms an upper bound on the exact

$$I_{0}^{(k)} = \sum_{\mathbf{m} \in \mathcal{M}^{(k)}} (-1)^{\widehat{m}^{(k)}} \frac{\lambda_{D}^{M_{E} - \widehat{m}^{(k)}} \exp\left(\frac{k}{\lambda_{D}}\right)}{\lambda_{E}^{M_{E}} k^{M_{E}} \left(\prod_{q=1}^{k} m_{q}!\right)} \times \left[\Gamma\left(0, \frac{k}{\lambda_{D}}\right) - \exp\left(\frac{1}{\lambda_{E}}\right) \sum_{t=1}^{M_{E}} \lambda_{E}^{t-M_{E}} \Gamma\left(-\left(M_{E} - t\right), \frac{k}{\lambda_{D}} \left(1 + \frac{\lambda_{D}}{k\lambda_{E}}\right)\right)\right].$$

$$I_{1}^{(k)} = \sum_{\mathbf{m} \in \mathcal{M}^{(k)}} \sum_{\mathbf{n} \in \mathcal{N}^{(k)}(\mathbf{m})} \sum_{v=0}^{\widehat{m}^{(k)} - \widehat{n}_{q}^{(k)} \widehat{n}_{q}^{(k)} + v - 1} (-1)^{\widehat{m}^{(k)} + \widehat{n}_{q}^{(k)} + v + i} \left(\widehat{m}^{(k)} - \widehat{n}_{q}^{(k)}\right) \left(\widehat{n}_{q}^{(k)} + v - 1\right) \times \frac{\Gamma(M_{E} + \widehat{n}_{q}^{(k)}) \left(\prod_{q=1}^{k} {m_{q} \choose n_{q}}\right) \Gamma\left(-\left(kM_{E} - v + i\right), \frac{k}{\lambda_{D}} \left(1 + \frac{\lambda_{D}}{k\lambda_{E}}\right)\right) \exp\left(\frac{k}{\lambda_{D}} + \frac{1}{\lambda_{E}}\right)}{\lambda_{D}^{\widehat{m}^{(k)} - \widehat{n}_{q}^{(k)} - v} \lambda_{E}^{M_{E} + i} k^{\widehat{n}_{q}^{(k)} + v} \left(\prod_{q=1}^{k} m_{q}!\right) \Gamma(M_{E})}$$

$$(66)$$

 $\Gamma_S^{(k,l)}.$ With this approximation, the high-SNR CDF of Γ_S is evaluated as

$$F_{\Gamma_S}(x) = \mathbb{P}\left[\max_{\forall k, \forall l} \left\{\gamma_D^{(k,l)}\right\} \le x \left(\gamma_E^{(k^*)}\right)\right]$$

$$= \int_0^\infty \left[F_{\gamma_D^{(k,l)}}(xy)\right]^{KL} f_{\gamma_E^{(k^*)}}(y) dy$$

$$= 1 - \sum_{k=1}^{KL} (-1)^{k+1} \binom{KL}{k} \Psi^k(x), \tag{67}$$

where $\Psi^k(x)$ is evaluated similar to (61) using (59) as

$$\Psi^{k}(x) = \sum_{\mathbf{m} \in \mathcal{M}^{(k)}} \frac{\lambda_{D}^{M_{E}} \Gamma\left(M_{E} + \widehat{m}^{(k)}\right)}{\lambda_{E}^{M_{E}} k^{M_{E} + \widehat{m}^{(k)}} \left(\prod_{q=1}^{k} m_{q}!\right) \Gamma\left(M_{E}\right)} \times \frac{x^{\widehat{m}^{(k)}}}{\left(x + \frac{\lambda_{D}}{k\lambda_{E}}\right)^{M_{E} + \widehat{m}^{(k)}}},$$
(68)

where

$$\Psi^{k}(x,y) = \left[\sum_{m=0}^{M_{D}-1} \frac{x^{m} y^{m} \exp\left(-\frac{xy}{\lambda_{D}}\right)}{(m!) \lambda_{D}^{m}}\right]^{k}$$

$$= \sum_{\mathbf{m} \in \mathcal{M}^{(k)}} \frac{x^{\widehat{m}^{(k)}} y^{\widehat{m}^{(k)}} \exp\left(-\frac{kxy}{\lambda_{D}}\right)}{\left(\prod_{q=1}^{k} m_{q}!\right) \lambda_{D}^{\widehat{m}^{(k)}}}.$$
 (69)

In the above expression, the product-of-sums is converted to the sum-of-products for integration using an approach similar to (16) as in the OS scheme. Next, the ESR can be expressed in the form of (62). In (62) for high-SNR approximation, $I_0^{(k)}$ corresponds to the condition $\widehat{m}^{(k)}=0$, with solution given in (70), while $I_1^{(k)}(x)$ corresponds to all other cases, i.e., $\widehat{m}^{(k)}\neq 0$, the solution of which is presented in (71).

Comparing (42) and (43) for the OS scheme with (70) and (71) for the SS scheme for L=1, respectively, we note that the ESR is a function of λ_D/λ_E in both selection schemes. However, we observe that the SNR ratio is lower in the SS scheme as it is decreased by the factor k number of transmitters. This intuitively relates to the fact that the SS

scheme achieves a lower average destination to eavesdropper channel SNR ratio per path than the OS scheme, and therefore its ESR performance suffers.

D. Asymptotic Analysis

As in Section III-D, the asymptotic analysis in SS is aimed at providing better insights regarding the relationship between the system parameters and the ESR. By approximating $1+\frac{\lambda_D}{k\lambda_E}\approx\frac{\lambda_D}{k\lambda_E}$ in (70) and (71) for all $k\in\{1,\ldots,K\}$, $I_0^{(k)}$ for the SS scheme in the asymptotic scenario is evaluated and expressed as in (72). Similarly, after performing some mathematical simplifications, we obtain $I_1^{(k)}$ as in (73).

$$I_0^{(k)} = \ln\left(\frac{\lambda_D}{k\lambda_E}\right) - H_{M_E - 1}.\tag{72}$$

$$I_1^{(k)} = \sum_{\mathbf{m} \in \mathcal{M}^{(k)}} \frac{\Gamma(\widehat{m}^{(k)})}{k^{\widehat{m}^{(k)}} \left(\prod_{q=1}^k m_q!\right)}.$$
 (73)

We also transform C_{erg}^{∞} into a linear function of $\log_2(\lambda_D)$ in the logarithmic scale as was done in (53) for the OS scheme. The slope \mathcal{S}_{∞} and the offset \mathcal{L}_{∞} for the SS scheme are evaluated as

$$\mathcal{S}_{\infty} = 1$$
, and
$$\mathcal{L}_{\infty} = \sum_{k=1}^{KL} (-1)^{k+1} {KL \choose k} \left[\log_2(k\lambda_E) + \frac{1}{\ln(2)} \psi_{\infty}^{(k)} \right], \quad (74)$$

where $\psi_{\infty}^{(k)}$ is expressed as

$$\psi_{\infty}^{(k)} = H_{M_E - 1} - I_1^{(k)}. (75)$$

We observe from the asymptotic analysis of the SS scheme that the slope is independent of all system parameters and is equal to unity, as in the OS scheme for L=1 in (54). The high-SNR offset depends on $\lambda_E,\,M_E,\,M_D$ and K. Further, it is clearly visible by comparing the results in (72) and (47) that the SS scheme achieves lower average destination to eavesdropper channel SNR per path ratio than the OS scheme, as was observed also in the high-SNR approximate analysis.

$$I_0^{(k)} = \ln\left(1 + \frac{\lambda_D}{k\lambda_E}\right) - \sum_{t=1}^{M_E - 1} \frac{\left(\frac{\lambda_D}{k\lambda_E}\right)^{M_E - t}}{\left(M_E - t\right)\left(1 + \frac{\lambda_D}{k\lambda_E}\right)^{M_E - t}}.$$
 (70)

$$I_1^{(k)} = \sum_{\mathbf{m} \in \mathcal{M}^{(k)}} \sum_{v=0}^{\widehat{m}^{(k)} - 1} (-1)^{\widehat{m}^{(k)} - v - 1} {\widehat{m}^{(k)} - 1 \choose v}$$

$$\times \frac{\left(\frac{\lambda_{D}}{k\lambda_{E}}\right)^{(M_{E}+\widehat{m}^{(k)}-v-1)}\Gamma(M_{E}+\widehat{m}^{(k)})}{\left(1+\frac{\lambda_{D}}{k\lambda_{E}}\right)^{(M_{E}+\widehat{m}^{(k)}-v-1)}k^{\widehat{m}^{(k)}}(M_{E}+\widehat{m}^{(k)}-v-1)\left(\prod_{q=1}^{k}m_{q}!\right)\Gamma(M_{E})}.$$
(71)

From (75) it is noted that even if $M_D=M_E$ when K,L>1, even the high-SNR offset is different for a different number of multipath components. This is the same as observed in the OS scheme for L=1, even though the values are different from those for the OS scheme. In the special case when K=1, the OS and SS scheme results are the same as there is no selection involved. For the case of Rayleigh fading, i.e., $M_D=M_E=1$ with an arbitrary $K,\,\psi_\infty^{(k)}=0$ as $H_0=0$ and $I_1^{(k)}=0$ in (74) ($I_1^{(k)}$ exists only for the condition $\widehat{m}^{(k)}\neq 0$). This substitution in (74) provides the slope as $\mathcal{S}_\infty=1$ and the high-SNR offset as

$$\mathcal{L}_{\infty} = \sum_{k=1}^{KL} (-1)^{k+1} {KL \choose k} \log_2(k\lambda_E)$$

$$= \log_2(\lambda_E) - \frac{1}{\ln(2)} \sum_{k=1}^{KL} (-1)^k {KL \choose k} \ln(k), \quad (76)$$

for the SS scheme. On comparing (76) and (56), it can be noted that since $H_{k-1} > \ln(k)$ for all $k \in \mathcal{S}$, the high-SNR offset in the OS scheme is greater than that of the SS scheme in the case of Rayleigh fading. This leads to improved performance in the OS scheme.

As on the application of SC-CP modulation, the underlying frequency selective fading channel behaves as a narrowband Nakagami-m fading channel with integer parameter m, the ESR results derived for the OS and SS schemes in this paper also provide the corresponding analysis for the case of narrowband channels with Nakagami-m fading channels. In this regard we observe that [2] considers the sub-optimal transmitter selection scheme over Nakagami-m fading channel with multiple antennas at the destination and eavesdropper using diversity combining. However, the source-destination pair selection is not present in [2]. Moreover, the methodology in [2] cannot be extended to analyze the OS scheme.

V. TRANSMITTER AND PATH CORRELATION

In this section we will describe the transmitter and path correlation models that will be adopted in our work. In Section VI we will use these correlation models together with our derived analytical results to study the effect of these correlations on the ESR performance. We will consider transmitter correlation, destination path correlation, and eavesdropper path correlation. The composite destination channel \mathbf{H}_D of size $L \times KM_D$, including all multipath components $i \in \{1,\ldots,M_D\}$ between

 S_k , for all $k \in \mathcal{S}$, and D_l , for all $l \in \mathcal{D}$, is generated following [19] by introducing transmitter and path correlation as

$$\mathbf{H}_D = \mathbf{H}_{\omega(L \times KM_D)} \left(\mathbf{R}_D^{T/2} \otimes \mathbf{R}_S^{1/2} \right), \tag{77}$$

where $\mathbf{H}_{\omega(L\times KM_D)}$ denotes the $L\times KM_D$ channel matrix with each element $h_{\omega}^{(k,l)}(i)$ is a circularly symmetric complex Gaussian random variable with zero mean and variance λ_D for all possible $k\in\{1,\ldots,K\},\ l\in\mathcal{D},\$ and $i\in\{1,\ldots,M_D\}.$ $\mathbf{H}_{\omega(L\times KM_D)}$ is denoted as

$$\mathbf{H}_{\omega(L\times KM_D)} = \begin{bmatrix} \mathbf{h}_{\omega}^{(1,1)} & \dots & \mathbf{h}_{\omega}^{(1,L)} \\ \vdots & \mathbf{h}_{\omega}^{(k,l)} & \vdots \\ \mathbf{h}_{\omega}^{(K,1)} & \dots & \mathbf{h}_{\omega}^{(K,L)} \end{bmatrix}^{\mathrm{T}}, \quad (78)$$

where $\mathbf{h}_{\omega}^{(k,l)} = \left[h_{\omega}^{(k,l)}(1), \dots, h_{\omega}^{(k,l)}(M_D)\right]^{\mathsf{T}}$. \mathbf{R}_S and \mathbf{R}_D are transmitter correlation and destination path correlation matrices of size $K \times K$ and $M_D \times M_D$, respectively. These are Toeplitz matrices with (i,j)-entry equal to

$$[\mathbf{R}_{D}]_{i,j} = \lambda_{D} \ \rho_{D}^{|i-j|}; \ \forall i, j \in \{1, \dots, M_{D}\},$$

$$[\mathbf{R}_{S}]_{i,j} = \rho_{S}^{|i-j|}; \ \forall i, j \in \{1, \dots, K\},$$
(79)

respectively, where ρ_D and ρ_S are correlation exponents with $0 \leq |\rho_D| \leq 1$ and $0 \leq |\rho_S| \leq 1$ [19]. In this scenario, $\mathbf{H}_D = [\mathbf{H}_1, \dots, \mathbf{H}_{M_D}]$ where $\mathbf{H}_i \in \mathbb{C}^{L \times K}$ denotes the channel matrix of the i^{th} path of S_k - D_l for all k and l. The correlation matrix between two different paths i and j ($i \neq j$) can be defined as

$$\mathbb{E}\left[\operatorname{vec}\{\mathbf{H}_{i}\} \operatorname{vec}\{\mathbf{H}_{j}\}^{\mathrm{H}}\right] = \lambda_{D} \rho_{D}^{|i-j|} \mathbf{R}_{S}^{\mathrm{T}}; \quad \forall i, j \in \{1, \dots, M_{D}\}.$$
(80)

 \mathbf{H}_D is structurally similar to (78) and we obtain \mathbf{H}_D by replacing ω in \mathbf{H}_ω with D. Similarly, the composite eavesdropping channel \mathbf{H}_E of size $1 \times KM_E$, including all multipath components $i \in \{1,\ldots,M_E\}$ between S_k and E for all $k \in \mathcal{S}$, is generated including transmitter and path correlations assuming the eavesdropping path correlation matrix to be a Toeplitz matrix $[\mathbf{R}_E]_{i,j} = \rho_E^{|i-j|}, \ \forall i,j \in \{1,\ldots,M_E\}$, where $0 \leq |\rho_E| \leq 1$, by suitably modifying (77)-(79).

Using channel realizations realizations based on \mathbf{H}_D and \mathbf{H}_E for all multipath components between S_k and D_l , and between S_k and E, respectively, for all $k \in \mathcal{S}$ and $l \in \mathcal{D}$, the simulation of ESR is performed by evaluating Γ_S in (10) for

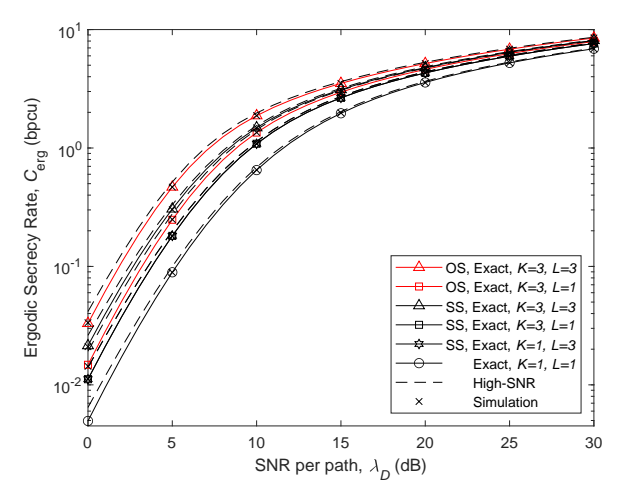


Fig. 2: Variation of exact ESR and its high-SNR approximation with λ_D for $M_D=M_E=3$ and $\lambda_E=9$ dB.

the OS scheme and (57) for the SS schemes and using (8).

VI. RESULTS

In this section, we provide analytical results along with the corresponding simulations except for Fig. 5 where only simulation results are plotted. Figs. 2-4 do not include transmitter or path correlation, whereas Fig. 5 includes both transmitter correlation and path correlation. The simulation results completely agree with the analysis in all these figures, thus validating the correctness of our analytical approach.

Fig. 2 depicts the ESR performance versus λ_D by changing the number of transmitters and destinations for the OS and SS schemes. The curve for K=L=1 serves as a reference to show the performance improvement with selection. We observe that the high-SNR approximate ESR is very close to the exact ESR. We also find that the increase in the number of transmitters or destinations improves the ESR performance due to the diversity benefit from the selection. As expected, the OS scheme has the best performance among the two schemes. It is noted that the ESR performance for $\{K, L\} = \{1, 3\}$ is the same for the OS and SS schemes as K = 1 means destination selection only. We also notice that with an increase in K from 1 to 3 any $L = \{1, 3\}$, the ESR performance improvement in the OS scheme is more significant than in the SS scheme. Furthermore, we observe that with an increase in L from 1 to 3, although the OS scheme outperforms the SS scheme for any $K = \{1, 3\}$, this advantage is not as significant as in the case of increasing K for a fixed value of L. These observations show that the OS scheme can take advantage of increasing both K and L, however, increasing K is better for the system security than increasing L in the OS scheme.

For the SS scheme, we notice that the ESR curves for $\{K,L\}=\{1,3\}$ and $\{K,L\}=\{3,1\}$ overlap. This is because in both the cases there are $K\times L=3$ available i.i.d. links from which to select the best source-destination pair. This also suggests that if the total number of links KL is the same for any combination of K and L, the ESR performance is the same for these combinations in the SS scheme. However, in contrast to the SS scheme, the curves for these combinations in

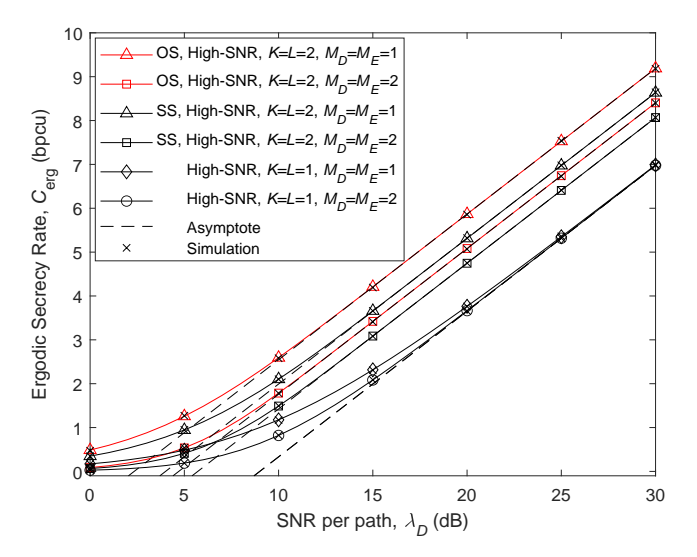


Fig. 3: Variation of high-SNR approximate ESR and its asymptotic performance with λ_D for $\lambda_E = 9$ dB.

the OS scheme do not overlap. The reason is that the selection takes into consideration the eavesdropper channel quality also, and hence does not provide the same source-destination pair at all times for these combinations. It is also noted that the SS scheme can be made to outperform the OS scheme by increasing the number of destinations only, thereby reducing the reliance on the eavesdropping channel feedback in the OS scheme, which may not be available for the selection.

Fig. 3 plots the high-SNR approximate ESR and its asymptotes with respect to λ_D for $K = L \in \{1, 2\}$ and $M_D =$ $M_E \in \{1,2\}$. As the high-SNR approximate ESR is very close to the exact ESR, only the approximate ESR curves are included in this figure for clarity of presentation. The asymptotes closely match with the ESR at high SNR, which validates our theoretical analysis. We observe that all the curves have the same slope of unity irrespective of the values of λ_E , K, L, M_D , and M_E . As the number of multipath components is increased while maintaining $M_D = M_E$, we find that the performance degrades in both selection schemes for given values of K and L. Also, we note that the performance in the case of $M_D = M_E = 1$ (i.e., for the Rayleigh fading condition) is the best for given values of K and L. For the case $M_D = M_E$, as the number of multipath components in both the destination and eavesdropper channel increase, the ESR performance always degrades. This shows that the performance of the selection schemes is dominated by M_E , or equivalently by the eavesdropping channel quality. The system with the worst eavesdropper channel (i.e., a Rayleigh fading channel to the eavesdropper) has the best ESR performance.

Furthermore, we observe that as λ_D improves, the ESR curves corresponding to different numbers of multipath components merge at high SNR when K=L=1. This is because the high-SNR offset for the asymptotic ESR in the case of K=L=1 for any $M_D=M_E$ is the same. This is not the case when K>1 and L>1; for example, it can be seen that for K=L=2, the curves for $M_D=M_E=1$

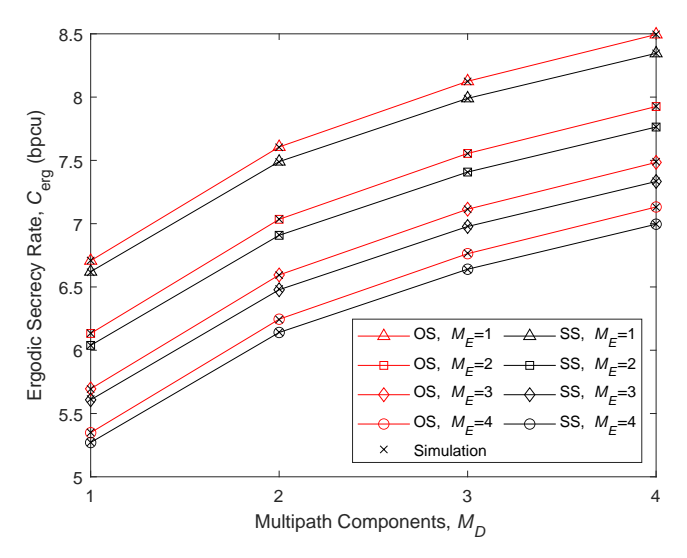


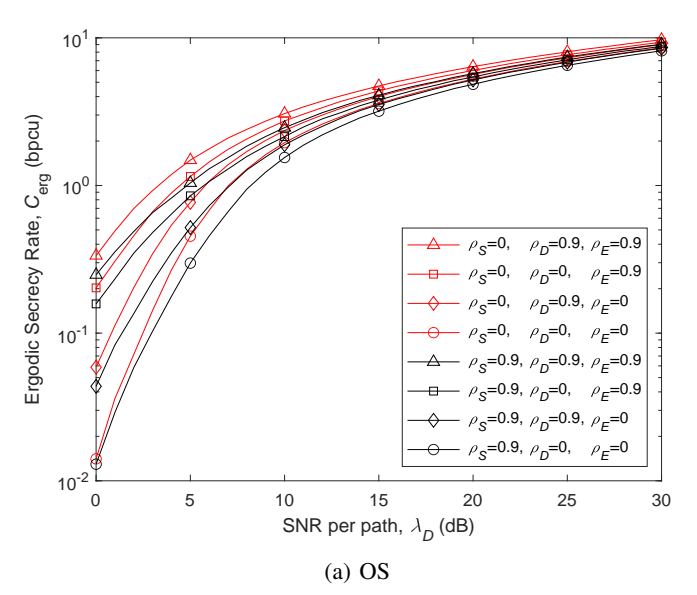
Fig. 4: Variation of exact ESR with M_D for K=L=2, $\lambda_E=0$ dB, and $\lambda_D=20$ dB.

and $M_D=M_E=2$ do not merge. These two observations corroborate our analysis regarding the high-SNR offset for any K and L=1 in the OS scheme and any K and L in the SS scheme provided in Section III-D and IV-D, respectively.

To understand the effect of the number of multipath components on the ESR, we show the variation of the ESR with M_D for different values of M_E at $K=L=2, \lambda_E=0$ dB and $\lambda_D = 20$ dB in Fig. 4. For a given set of parameters, as we increase M_D , the ESR increases, whereas an increase in M_E causes a decrease in the ESR. This occurs because an increase in M_D and M_E increases the received SNR at D and E, respectively, due to the improvement in the corresponding channel quality. Further, the performance gap between the OS and SS schemes also improves with increasing M_D , though very slowly. The performance gap between the OS and SS schemes also increases with a decrease in M_E . This suggests that the OS scheme can take better advantage of the eavesdropping quality degradation. As $M_E = 1$ corresponds to a Rayleigh faded eavesdropper channel, this condition represents the worst possible channel for an eavesdropper. These observations suggest that the OS scheme is more sensitive to the variation in M_E than the variation in M_D .

Fig. 5 shows the ESR performance versus λ_D for different levels of transmitter correlation and path correlation for the OS and SS schemes. Curves in red color represent a system without transmitter correlation, while curves in black color include transmitter correlation with correlation coefficient $\rho_S=0$ and $\rho_S=0.9$, respectively. In both cases, the correlation between paths towards destinations and eavesdroppers are varied. It is observed that as the transmitter correlation coefficient is increased from $\rho_S=0$ to $\rho_S=0.9$, the ESR performance degrades. It can be observed that the effect of transmitter correlation is greater in the OS scheme in Fig. 5a as compared to the SS scheme in Fig. 5b.

We notice from the figure that increasing the destination path correlation (ρ_D) improves the ESR performance. This is a result of power focusing at the destination which happens due



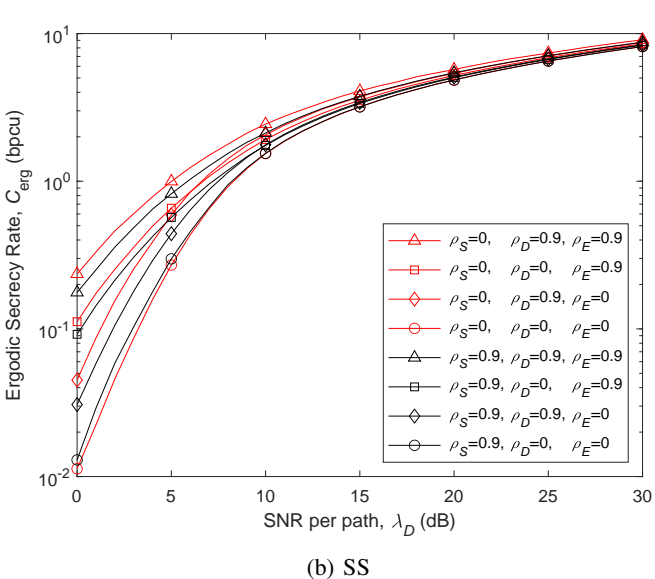


Fig. 5: Variation of exact ESR with λ_D for K=L=4, $M_D=M_E=4$, and $\lambda_E=9$ dB.

to the reduced effective dimensionality when correlation increases. Effective dimensionality reduction was also observed in [17] in the case of increased destination antenna correlation, however, in a Nakagami flat fading channel. The performance improvement reduces with increasing λ_D as all the curves merge at high SNR. This indicates that at high SNR, effective dimensionality reduction is insignificant. We also find that an increase in the eavesdropper path correlation (increasing ρ_E) improves secrecy performance. This observation is also similar to that observed in [17] where eavesdropper antenna correlation is increased. Though an increase in both ρ_D and ρ_E improves secrecy performance, we notice that an increase in ρ_E is better for secrecy as the gap between plots for $\rho_E = 0$ and $\rho_E = 0.9$ is higher than that of the gap between plots of $\rho_D = 0$ and $\rho_D = 0.9$ in both the OS and SS schemes, irrespective of the value of ρ_S .

VII. CONCLUSION

In this paper, the ESR of optimal and sub-optimal sourcedestination pair selection schemes is evaluated in closed form for a system with multiple transmitters, multiple destinations, and a single eavesdropper in frequency selective fading channels with SC-CP signaling. We also demonstrate numerically the effect of transmitter correlation along with destination and eavesdropper path correlation. A high-SNR analysis along with an asymptotic analysis has been provided in order to yield a low-complexity ESR evaluation and to provide key insights. Our analysis also provides the corresponding ESR results in narrowband Nakagami fading channels with arbitrary integer parameter m. Our proposed analysis is general and can also be used to evaluate the ESR of other sub-optimal selection schemes already available in the literature. We notice that for any given combination of the number of transmitters and destinations, the highest ESR is achieved under Rayleigh fading conditions irrespective of the selection schemes. We also find that the OS scheme can take better advantage of the multipath conditions in the system. We observe that for the OS scheme, it is better to increase the number of transmitters than destinations for the improvement of the ESR, while on the other hand, in case of the SS scheme, the ESR shows the same dependence on the number of transmitters as on the number of destinations. We also observe that while transmitter correlation deteriorates the ESR, destination and eavesdropper path correlation both improve it.

APPENDIX

A. Evaluation of $J_0^{(k)}$ in (24).

In the denominator of (24), the values of l_q for different $q \in \{1,\ldots,k\}$ may be the same or different. We denote by $\mathcal I$ the number of distinct values of l_q that are taken on more than once. We also define $\mathcal Q_i$, where $i \in \{1,\ldots,\mathcal I\}$, as the set of indices q for which l_q takes the i^{th} distinct value. We also define $\mathcal Q = \mathcal Q_1 \cup \mathcal Q_2 \cup \ldots, \mathcal Q_{\mathcal I}$ and $\bar{\mathcal Q} = \{1,\ldots,k\} - \mathcal Q$.

Note that when the values of l_q for each $q \in \{1, ..., k\}$ are distinct, $\bar{\mathcal{Q}}$ is an empty set. Using the above notations, the partial fraction expansion of the integrand in (24) is obtained, and then the solution is obtained with the help of the integral solution [25, eq. (3.462.16) and (3.462.19)] as

$$J_0^{(k)} = \int_1^\infty \left(\frac{A \exp(-\frac{\tilde{l}^{(k)}}{\lambda_D} x)}{x} + \sum_{i=1}^{\mathcal{I}} \sum_{\substack{t=1 | q \in \mathcal{Q}_i \\ t = 1}}^{|\mathcal{Q}_i|M_E + \sum_{q \in \mathcal{Q}_i} \hat{n}_q^{(l_q)}} \frac{B_{i,t} \exp(-\frac{\tilde{l}^{(k)}}{\lambda_D} x)}{\left(x + \frac{\lambda_D}{l_q \lambda_E}\right)^t} + \sum_{q \in \tilde{\mathcal{Q}}_i} \sum_{t=1}^{M_E + \hat{n}_q^{(l_q)}} \frac{C_{q,t} \exp(-\frac{\tilde{l}^{(k)}}{\lambda_D} x)}{\left(x + \frac{\lambda_D}{l_q \lambda_E}\right)^t} \right) dx.$$
(81)

The coefficients A, $B_{i,t}$ and $C_{q,t}$ are evaluated using the method of partial fractions. The second term in (81) corresponds to the case of values l_q that appear more than once, while the third term corresponds to the case of of values of l_q that appear exactly once. For given values of K, L, M_D ,

 M_E , the partial fraction coefficients A, $B_{i,t}$ and $C_{q,t}$ are easily obtained.

B. Evaluation of $J_1^{(k)}$ in (25).

The solution of $J_1^{(k)}$ in (25) also depends on how many l_q for different $q \in \{1,\ldots,k\}$ in the denominator of (25) are equal, as in (24) for $J_0^{(k)}$. In addition, the solution method also needs to take care that the power of x in the numerator of (25) may be greater than the highest power of x in the denominator; note that this was not an issue for $J_0^{(k)}$ in (24). The solution method is to first check whether all l_q are equal to each other in (25); if they are all equal, no partial fraction is required. We then adopt a change of variable taking into account that the power of x in the numerator can be greater than that in the denominator. Finally, using the integration solution [25, eq. (3.351.2)] we obtain the solution as

$$J_{1}^{(k)} = \sum_{j=0}^{\widetilde{m}^{k} - \widetilde{u}^{k} - 1} {\widetilde{m}^{k} - \widetilde{u}^{k} - 1 \choose j}$$

$$\times \left(-\frac{\lambda_{D}}{l_{q}\lambda_{E}} \right)^{\widetilde{m}^{k} - \widetilde{u}^{k} - 1 - j} \exp\left(\frac{\widetilde{l}^{(k)}}{l_{q}\lambda_{E}} \right)$$

$$\times \int_{1 + \frac{\lambda_{D}}{l_{q}\lambda_{E}}}^{\infty} z^{j - (kM_{E} + \sum_{q=1}^{k} \widehat{n}_{q}^{(l_{q})})} \exp\left(-\frac{\widetilde{l}^{(k)}}{\lambda_{D}} z \right) dz. \tag{82}$$

In the case where the l_q values for distinct $q \in \{1, ..., k\}$ are not all equal in (25), we use partial fractions without including the numerator. The partial fraction method is similar to that used in (81). Then we adopt a change of variable similar to (82) and subsequently use the integration solution [25, eq. (3.351.2)] to obtain the solution as

$$J_{1}^{(k)} = \sum_{i=1}^{\mathcal{I}} \sum_{t=1|q \in \mathcal{Q}_{i}}^{|\mathcal{Q}_{i}|M_{E} + \sum_{q \in \mathcal{Q}_{i}} \widehat{n}_{q}^{(l_{q})} \widetilde{m}^{k} - \widetilde{u}^{k} - 1} \exp\left(\frac{\widetilde{l}^{(k)}}{l_{q}\lambda_{E}}\right)$$

$$\times \left(\widetilde{m}^{k} - \widetilde{u}^{k} - 1\right) \left(-\frac{\lambda_{D}}{l_{q}\lambda_{E}}\right)^{\widetilde{m}^{k} - \widetilde{u}^{k} - 1 - j} B_{i,t}$$

$$\times \int_{1 + \frac{\lambda_{D}}{l_{q}\lambda_{E}}}^{\infty} z^{j-t} \exp\left(-\frac{\widetilde{l}^{(k)}}{\lambda_{D}}z\right) dz$$

$$+ \sum_{q \in \widetilde{\mathcal{Q}}} \sum_{t=1}^{M_{E} + \widehat{n}_{q}^{(l_{q})}} \sum_{j=0}^{\widetilde{m}^{k} - \widetilde{u}^{k} - 1} \exp\left(\frac{\widetilde{l}^{(k)}}{l_{q}\lambda_{E}}\right)$$

$$\times \left(\widetilde{m}^{k} - \widetilde{u}^{k} - 1\right) \left(-\frac{\lambda_{D}}{l_{q}\lambda_{E}}\right)^{\widetilde{m}^{k} - \widetilde{u}^{k} - 1 - j} C_{q,t}$$

$$\times \int_{1 + \frac{\lambda_{D}}{1 - \lambda_{D}}}^{\infty} z^{j-t} \exp\left(-\frac{\widetilde{l}^{(k)}}{\lambda_{D}}z\right) dz. \tag{83}$$

Here, \mathcal{I} , \mathcal{Q}_i , and $\bar{\mathcal{Q}}$ have same definition as in (81), however, the partial fraction coefficients $B_{i,t}$ and $C_{q,t}$ are specific to $J_1^{(k)}$. These coefficients are evaluated in a similar manner to (81).

C. Evaluation of $J_1^{(k)}$ in (38) at high SNR.

When all l_q are equal for all $q \in \{1, ..., k\}$, the solution of $J_1^{(k)}$ in (38) at high SNR is evaluated easily, as the highest

power of x in the numerator is always smaller than the highest power of x in the denominator. Integration is evaluated after a change of variable as

$$J_1^{(k)} = \int_1^\infty \frac{x^{\tilde{m}^{(k)} - 1}}{\left(x + \frac{\lambda_D}{l_q \lambda_E}\right)^{k M_E + \tilde{m}^{(k)}}} dx.$$
 (84)

When any l_q is distinct for any $q \in \{1, \dots, k\}$, $J_1^{(k)}$ in (38) at high SNR is evaluated by adopting the partial fraction method similar to (39) as

$$J_{1}^{(k)} = \int_{1}^{\infty} \left(\sum_{i=1}^{\mathcal{I}} \sum_{t=1|q \in \mathcal{Q}_{i}}^{|\mathcal{Q}_{i}|M_{E} + \sum_{q \in \mathcal{Q}_{i}} \widehat{m}_{q}^{l_{q}}} \frac{B_{i,t}}{\left(x + \frac{\lambda_{D}}{l_{q}\lambda_{E}}\right)^{t}} + \sum_{q \in \bar{\mathcal{Q}}_{i}} \sum_{t=1}^{M_{E} + \widehat{m}_{q}^{l_{q}}} \frac{C_{q,t}}{\left(x + \frac{\lambda_{D}}{l_{q}\lambda_{E}}\right)^{t}} \right) dx.$$
 (85)

The partial fraction coefficients $B_{i,t}$ and $C_{q,t}$ are obtained using the standard partial fraction technique.

REFERENCES

- H. V. Poor, M. Goldenbaum, and W. Yang, "Fundamentals for IoT networks: Secure and low-latency communications," in *Proc. 2nd Inter*national Conference on Recent Advances in Signal Processing, Telecommunications Computing, Bangalore, India, Jan. 2019, pp. 362–364.
- [2] L.Wang, M. Elkashlan, J. Huang, R. Schober, and R. K. Mallik, "Secure transmission with antenna selection in MIMO Nakagami-m fading channels," *IEEE Transactions on Wireless Communications*, vol. 13, no. 11, pp. 6054–6067, Nov. 2014.
- [3] S. Thakur and A. Singh, "Ergodic secrecy capacity in Nakagamim fading channels," in *Proc. International Carnahan Conference on Security Technology*, Chennai, India, Oct. 2019, pp. 1–3.
- [4] R. Zhao, H. Lin, Y. C. He, D. H. Chen, Y. Huang, and L. Yang, "Secrecy performance of transmit antenna selection for MIMO relay systems with outdated CSI," *IEEE Transactions on Communications*, vol. 66, no. 2, pp. 546–559, Feb. 2018.
- [5] K. J. Kim, P. L. Yeoh, P. V. Orlik, and H. V. Poor, "Secrecy performance of finite-sized cooperative single carrier systems with unreliable backhaul connections," *IEEE Transactions on Signal Processing*, vol. 64, no. 17, pp. 4403–4416, Sep. 2016.
- [6] C. Kundu, S. Ghose, and R. Bose, "Secrecy outage of dual-hop regenerative multi-relay system with relay selection," *IEEE Transactions on Wireless Communications*, vol. 14, no. 8, pp. 4614–4625, Aug. 2015.
- [7] C. Kundu, T. M. N. Ngatched, and O. A. Dobre, "Relay selection to improve secrecy in cooperative threshold decode-and-forward relaying," in *Proc. IEEE Global Communications Conference*, Washington, DC, USA, Dec. 2016, pp. 1–6.
- [8] J. Zhang, C. Kundu, O. A. Dobre, E. Garcia-Palacios, and N. Vo, "Secrecy performance of small-cell networks with transmitter selection and unreliable backhaul under spectrum sharing environment," *IEEE Transactions on Vehicular Technology*, vol. 68, no. 11, pp. 10895– 10908 Nov 2019
- [9] S. Tripathi, C. Kundu, O. A. Dobre, A.Bansal, and M. F. Flanagan, "Recurrent neural network assisted transmitter selection for secrecy in cognitive radio network," in *Proc. IEEE Global Communications Conference*, Taipei, Taiwan, Dec. 2020, pp. 1–6.
- [12] K. J. Kim, H. Liu, M. Wen, P. V. Orlik, and H. V. Poor, "Secrecy performance analysis of distributed asynchronous cyclic delay diversitybased cooperative single carrier systems," *IEEE Transactions on Communications*, vol. 68, no. 5, pp. 2680–2694, Jun. 2020.

- [10] C. Kundu and M. F. Flanagan, "Ergodic secrecy rate of optimal source selection in a multi-source system with unreliable backhaul," *IEEE Wireless Communications Letters*, vol. 10, no. 5, pp. 1118–1122, Feb. 2021.
- [11] S. B. Kotwal, C. Kundu, S. Modem, A. Dubey, and M. F. Flanagan, "Transmitter selection for secrecy in a frequency selective fading channel with unreliable backhaul," in *Proc. IEEE Vehicular Technology Confer*ence, Helsinki, Finland, Jun. 2021, pp. 1–7.
- [13] L. Wang, K. J. Kim, T. Q. Duong, M. Elkashlan, and H. V. Poor, "Security enhancement of cooperative single carrier systems," *IEEE Transactions on Information Forensics and Security*, vol. 10, no. 1, pp. 90–103, Jan. 2015.
- [14] H. Liu, P. L. Yeoh, K. J. Kim, P. V. Orlik, and H. V. Poor, "Secrecy performance of finite-sized in-band selective relaying systems with unreliable backhaul and cooperative eavesdroppers," *IEEE Journal on Selected Areas in Communications*, vol. 36, no. 7, pp. 1499–1516, Jul. 2018.
- [15] H. T. Nguyen, J. Zhang, N. Yang, T. Q. Duong, and W. Hwang, "Secure cooperative single carrier systems under unreliable backhaul and dense networks impact," *IEEE Access*, vol. 5, pp. 18310–18324, Jul. 2017.
- [16] J. Tubbax, B. Come, L. Van der Perre, L. Deneire, S. Donnay, and M. Engels, "OFDM versus single carrier with cyclic prefix: a systembased comparison," in *Proc. IEEE Vehicular Technology Conference*., NJ, USA, Oct. 2001, pp. 1115–1119.
- [17] N. Yang, H. A. Suraweera, I. B. Collings, and C. Yuen, "Physical layer security of TAS/MRC with antenna correlation," *IEEE Transactions on Information Forensics and Security*, vol. 8, no. 1, pp. 254–259, Jan. 2013
- [18] J. Si, H. Rong, Z. Cheng, Z. Li, J. Cheng, and C. Zhong, "Impact of channel correlation on secrecy performance over rayleigh fading channels," in *Proc. International Conference on Communications*, Shanghai, China, May. 2019, pp. 1–6.
- [19] E. Yoon, J. Hansen, and A. Paulraj, "Space-frequency precoding with space-tap correlation information at the transmitter," *IEEE Transactions* on *Communications*, vol. 55, no. 9, pp. 1702–1711, Sep. 2007.
- [20] I. Hammerstrom, M. Kuhn, and A. Wittneben, "Channel adaptive scheduling for cooperative relay networks," in *Proc. IEEE Vehicular Technology Conference*, Los Angeles, CA, USA, Sep. 2004, pp. 2788
- [21] Y. Zou, X. Wang, and W. Shen, "Physical-layer security with multiuser scheduling in cognitive radio networks," *IEEE Transactions on Commu*nications, vol. 61, no. 12, pp. 5103–5113, Dec. 2013.
- [22] Y. Zou, J. Zhu, X. Wang, and V. C. Leung, "Improving physical-layer security in wireless communications using diversity techniques," *IEEE Network*, vol. 29, no. 1, pp. 42–48, Jan. 2015.
- [23] S. Ghose, C. Kundu, and O. A. Dobre, "Secrecy outage of proactive relay selection by eavesdropper," in *Proc. Global Communications Conference*, Singapore, Dec. 2017, pp. 1–6.
- [24] M. A. Khan and A. U. H. Sheikh, "Equivalence between Nakagami channels and Rayleigh channels with diversity," in *Proc. Mosharaka International Conference on Communications, Signals and Coding*, Amman, Jordan, Oct. 2008, pp. 83–88.
- [25] I. S. Gradshteyn and I. M. Ryzhik, Table of Integrals, Series, and Products, 7th ed. San Diego, CA, USA: Academic, 2007.
- [26] A. D. Wyner, "The wire-tap channel," The Bell System Technical Journal, vol. 54, no. 8, pp. 1355–1387, Oct. 1975.
- [27] S. Yan, G. Geraci, N. Yang, R. Malaney, and J. Yuan, "On the target secrecy rate for SISOME wiretap channels," in *IEEE International Conference on Communications*, Sydney, Australia, Jun. 2014, pp. 987–992.
- [28] L. Wang, N. Yang, M. Elkashlan, P. L. Yeoh, and J. Yuan, "Physical layer security of maximal ratio combining in two-wave with diffuse power fading channels," *IEEE Transactions on Information Forensics* and Security, vol. 9, no. 2, pp. 247–258, Jan. 2014.